NATURAL RESOURCES

Geologic Map of the Sedro-Woolley North and Lyman 7.5-minute Quadrangles, Western Skagit County, Washington

by Joe D. Dragovich,
David K. Norman,
Thomas J. Lapen,
and Garth Anderson

Electron microprobe analysts
(Ar-Ar age dating in progress)
A. Johnson and L. Snee

Geochemical analysts
C. M. Knaack and D. M. Johnson

Cartography
Keith Ikerd

WASHINGTON
DIVISION OF GEOLOGY
AND EARTH RESOURCES

Open File Report 99-3
December 1999

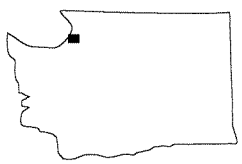

Location of quadrangles

WASHINGTON STATE DEPARTMENT OF
Natural Resources
Jennifer M. Belcher - Commissioner of Public Lands

Geologic Map of the Sedro-Woolley North and Lyman 7.5-minute Quadrangles, Western Skagit County, Washington

by Joe D. Dragovich,
David K. Norman,
Thomas J. Lapen,
and Garth Anderson

WASHINGTON
DIVISION OF GEOLOGY
AND EARTH RESOURCES

Open File Report 99-3
December 1999

Produced in cooperation with the U.S. Geological Survey
National Cooperative Geologic Mapping Program
Agreement Number 98-HQ-AG-2026

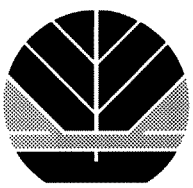

WASHINGTON STATE DEPARTMENT OF
Natural Resources
Jennifer M. Belcher - Commissioner of Public Lands

Contents

APPENDICES

ILLUSTRATIONS

PLATES *(accompany text)*

Geologic Map of the Sedro-Woolley North and Lyman 7.5-minute Quadrangles, Western Skagit County, Washington

Joe D. Dragovich, David K. Norman, Thomas J. Lapen, and Garth Anderson
Washington Department of Natural Resources
Division of Geology and Earth Resources
PO Box 47007; Olympia, WA 98504-7007

This report consists of geologic maps and cross sections (Plates 1, 2, 3, and 4) of the Sedro-Woolley North and Lyman 7.5-minute quadrangles in the Bellingham 30- by 60-minute quadrangle (Fig. 1). See Dragovich and others (in press b) for a companion report with additional data, observations, and an interpretation of the geologic history of the study area and surrounding areas.

Geologic units in this study are grouped broadly into Holocene laharic deposits, Holocene alluvium and miscellaneous mass-wastage deposits, Pleistocene glacial deposits, and Eocene sedimentary and pre-Tertiary metamorphic rocks (bedrock in Fig. 2). The Sedro-Woolley North and Lyman quadrangles are in the western portion of the Northwest Cascades system of Brown (1987) and contain a diversity of pre-Tertiary lithologic packages that are bounded by mid-Cretaceous thrust faults.

METHODS, PREVIOUS WORK, AND RELATED STUDIES

Our mapping is based on field work done in 1998 and 1999. Previous work in and adjacent to the Sedro-Woolley North and Lyman quadrangles is shown in Figure 3 or cited in the text.

Figure 4 shows the location of samples obtained for petrographic examination, as well as geochemical and ^{14}C age sample locations. Our petrographically determined mineral and clast abundance, textural, and other data are presented in the text. (Also see appendixes 1 and 2 of Dragovich and others, in press b, for additional point count data of glacial and nonglacial Quaternary geologic units.) We (Dragovich and Grisamer, 1998) compiled data from water wells and geotechnical borings (1,400 water well logs and about 80 geotechnical borings logs) in and adjacent to the Bow and Alger quadrangles, including the westernmost portion of the Sedro-Woolley North quadrangle. For our subsurface analysis, we examined approximately 1,200 water well logs and geotechnical boring logs. (See well and boring locations in Figure 5.)

We supplemented our field mapping with Washington State Department of Natural Resources (DNR) color 1:24,000-scale (1976) and black and white ~1:13,000-scale (1994) aerial photos. We also used 1991 DNR 1:12,000-scale orthophotos and 1944 U.S. Army 1:20,000 aerial photos (archived at DNR) to map surficial deposits, bedrock contacts, terraces, channel morphology, and lineaments.

Our mapping was compared with the soil unit boundaries mapped by Klungland and McArthur (1989). We slightly modified a few contacts on the basis of the soil parent material information provided by U.S. Soil Conservation Service maps. We supplemented our analyses with inspection of the 1917 U.S. Geological Survey (USGS) 1:63,500 topographic map as well as the initial 1880 State Land Survey planimetric map. Our field topographic base maps were developed from aerial photographs flown in 1989 and field checked in 1993 and thus show past Skagit River channel positions. All of these sources, as well as the aerial photograph base maps for the soil survey (1989), provided geomorphic information on the position of recently active Skagit River channels (Plate 3) as well as the location of abandoned channels and lateral accretion surfaces (Plate 1).

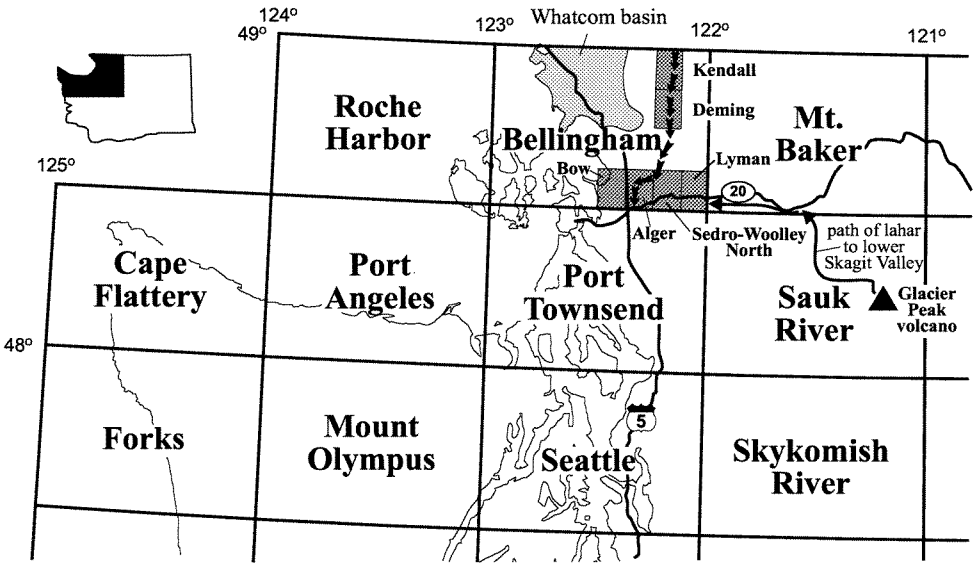

Figure 1. Locations of 1:100,000-scale quadrangles and past and current STATEMAP 7.5-minute mapping projects (darker pattern), northwestern Washington. See Dragovich and others (1997b) for the geologic maps and interpreted geologic history of the Kendall and Deming 1:24,000-scale quadrangles. Short arrows show the Sumas Stade outwash path through the foothills of the northwestern Cascade mountains (Easterbrook, 1979). The Sumas ice front near the Canadian border may have fed a braided river system that followed major south-trending valleys. Long arrows show the path of lahars (volcaniclastic mudflows) entering the lower Skagit River valley from past Glacier Peak volcanic events.

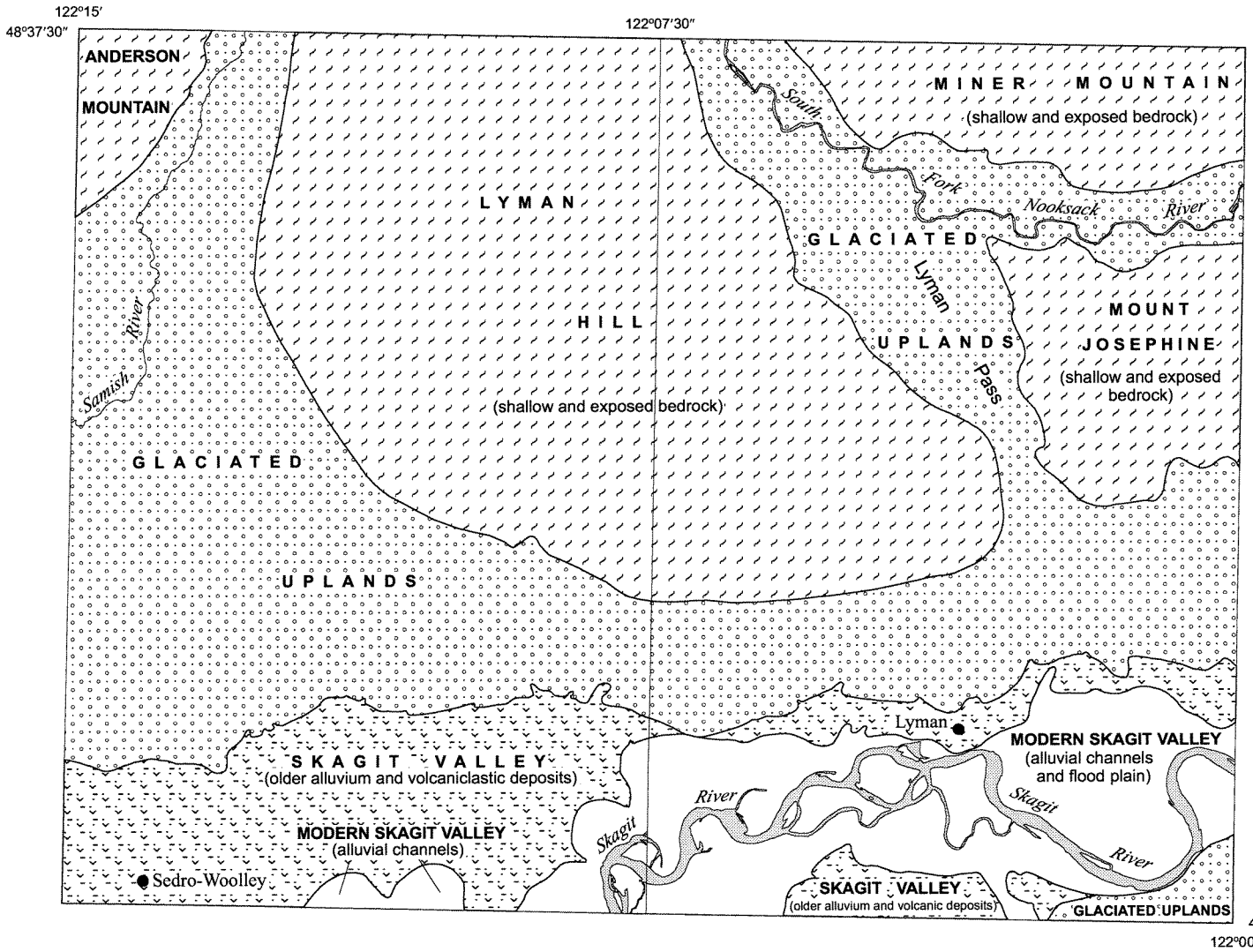

Figure 2. Location of shallow and exposed bedrock and Quaternary geologic-geomorphic domains of the study area. The mountains in the study area (for example, Lyman Hill) are locally veneered by Vashon glacial till and Everson recessional outwash. The glaciated uplands are typically separated from the Skagit valley alluvial channels, older alluvium, and volcanogenic deposits by a distinct scarp. Another prominent scarp also typically separates the modern Skagit River flood plain and channels from the older alluvium and volcanogenic deposits. Referenced geographic mountain names in the quadrangles are mostly informal. Lyman Hill is sometimes referred to as 'Lyman Mountain' in the literature. Mount Josephine proper is directly east of the study area.

DESCRIPTIONS OF MAP UNITS

Unit symbols provide information about the age, lithology, and name (if any) of the units: uppercase letters indicate protolith age, lowercase letters indicate lithology, and subscripts identify named units. For example, Jurassic Darrington Phyllite is shown with the symbol Jph_d. We used the geologic time scale devised for the "Correlation of Stratigraphic Units of North America (COSUNA)" project of the American Association of Petroleum Geologists (Salvador, 1985). Absolute ages of Cretaceous stage boundaries are from Obradovich (1994). Plutonic rocks are named according to their modal compositions using the International Union of Geological Sciences rock classification (Streckeisen, 1973). Some of the volcanic rocks are named using whole-rock geochemistry and the total alkali-silica diagram (Zanettin, 1984; Le Bas and others, 1986). Sandstones are named using the classification scheme of Folk (1980) or Dickinson (1970). Low-grade metamorphic rocks, including blueschist facies rocks, are described as metasedimentary or metavolcanic rocks (for example, metashale or metamorphosed shale or the equivalent metamorphic rock name 'phyllite'); rocks metamorphosed to less than greenschist facies are included in sedimentary, volcanic, or intrusive rock units (for example, siltstone or basalt). Landslides are classified using the terminology developed by Varnes (1958, 1978).

Quaternary Sedimentary and Volcanic Deposits

NONGLACIAL DEPOSITS

(Low-density deposits generally described as loose or soft)

Qa **Alluvium of the Skagit River valley, undivided (Holocene)**—Generally well-stratified and well-sorted fluvial deposits of cobbly gravel, gravel, sandy gravel, gravelly sand, and sand with overbank silt and clay; contains minor lacustrine sediments; clasts rounded to subrounded and derived from volcanic, metamorphic, and plutonic bedrock from the upper part of the Skagit drainage, as well as reworked laharic and glacial deposits; sands are micaceous (2–7%) and

contain microlitic volcanic fragments (16–30%), hypersthene (2–3%), and hornblende (2–3%)(see sand clast compositional data in appendix 1 of Dragovich and others, in press b); sands are shades of olive gray and have a 'salt and pepper' appearance as a result of the mixture of dark lithic clasts and opaque minerals with light-colored quartz, feldspar and intermediate volcanic lithic clasts, including probable microlitic volcanic dacite. (See unit Qoa and Dragovich and others, in press b, for further unit compositional information.) Gravel and cobble clast compositions are phyllite (15–25%); red, black, and gray vesicular to pumiceous porphyritic volcanic rocks (20–30%, mostly of intermediate composition); granitic rock and orthogneiss (10–20%); as well as vein quartz, quartzite and foliated metamorphic rocks (5–20%) and miscellaneous clasts (15–25%). Minor red porphyritic volcanic clasts are conspicuous in the gravelly alluvium. Many of these clasts may be reworked from the latest Pleistocene Crystal Creek lahar of Beget (1982). This lahar is found in the White Chuck and Sauk River valleys near the Glacier Peak volcano and contains abundant hydrothermally altered red clasts.

Water well, geotechnical boring, and field information shows that alluvium commonly contains upward-fining sequences 20 to 40 ft thick. Vertical sequences generally grade upward from coarse channel deposits to fine overbank deposits and are interpreted as the result of lateral migration of point bars, locally capped by flood or slack-water deposits. To the west, these fluvial deposits overlie Holocene deltaic and estuarine deposits of ancient Samish Bay. Late glacial deposits and (or) older alluvium (unit Qoa) underlie modern alluvium in the study area (Plate 3, cross sections A and B). Alluvium thickness ranges from a 20-ft veneer on shallowly buried glacial paleotopography to more than 250 ft elsewhere in the lower Skagit valley. A gravity study in the Lyman area by Foxall (1976) suggests that Holocene Skagit valley fill may be locally more than 500 ft thick. However, low-density materials in Foxall's geophysical model probably include late glacial Everson Interstade marine deposits. Thus we suggest that the maximum thickness of Holocene fill in the study area is substantially less than 500 ft.

Abandoned channels in the Skagit River valley appear as distinct to faint traces on aerial photos. These ancient channels are commonly associated with arcuate lateral accretion surfaces formed along meander bends of the ancestral Skagit River (Plate 1). Plate 3 shows a time-series map of the 1880–1993 Skagit River channel positions. The Skagit River channels and flood plains are bordered by older alluvium and 30- to 50-ft-high terraces (Fig. 2 and Plate 1). Channels change position by a combination of meandering and flood-induced channel avulsion. Although the data suggest that Skagit River channels are constrained between the elevated terraces, catastrophic floods are not. Silty flood deposits occur on the terraces and the record of historic flooding provides evidence of terrace inundation. (See Kunzler, 1991, for an informal discussion of the flood history of the Skagit River valley.)

Qa_s **Alluvium of the Samish River valley, undivided (Holocene)**—Generally consists of well-stratified and well-sorted deposits of clay, silt, silty sand, and locally peat, with lesser cobbly sandy gravel and gravelly sand. Clasts are rounded to subrounded, derived from local metamorphic rocks and reworked glacial deposits, and brown to gray in color, depending on oxidation state and composition. This unit is dominated by fine overbank deposits containing lenses of fluvial channel sand and gravel and locally interfingers with alluvial fan deposits (unit Qaf)(Plate 4, cross section F). It commonly overlies Sumas Stade and Everson Interstade glacial deposits at a fairly shallow depth (Plate 3, cross section D) and ranges from a 4-ft veneer to a maximum estimated thickness of 50 ft.

Qa_{sf} **Alluvium of the South Fork Nooksack River, undivided (Holocene)**—Moderately to poorly stratified, well- to moderately sorted sand, sandy gravel, cobble gravel, and bouldery cobble gravel with lesser silt. Clasts are generally subangular to subrounded, derived from local metamorphic rocks and reworked glacial deposits, and brown to gray in color, depending on oxidation state and composition; sand is grayish olive when dried, as a result of the abundance of olivine.

Alluvium is commonly interlayered with alluvial fan deposits (unit Qaf). One alluvial sand sample (appendix 1 of Dragovich and others, in press b) contains olivine (15%) and orthopyroxene and clinopyroxene (9%) of Twin Sisters Dunite origin; most other clasts reflect the bedrock composition of the Northwest Cascade system in the upper part of the drainage basin.

Alluvium overlies Vashon-age advance glacial-lake deposits and outwash, Evans Creek Stade alpine till, and bedrock; abundant outcrops of glacial strata in and near the modern channel provide evidence that the unit is typically a few feet to tens of feet thick. We term the alpine-till outcroppings at or below high river level as 'till pavement' (unit Qat_{ec}). In the South Fork Nooksack valley, loose boulder cobble gravel commonly caps 5- to 40-ft-high erosional terraces composed of glacial deposits. These uppermost alluvial strata are generally only 5 to 10 ft thick. We interpret these perched units as local occurrences of alluvium abandoned during Holocene South Fork incision. In order to emphasize the underlying glacial stratigraphy of the South Fork Nooksack River (for example, Plate 4, cross section H), we did not map this uppermost unit Qa_{sf} stratum (Plate 1).

Qvl, Qoa **Lahar and older volcanogenic alluvium and overbank deposits, undivided (Holocene)**—Unit consists of: (1) undivided interlayered probable lahar(?) diamicton (unit Qvl) and (2) pumiceous or vesicular dacite-clast-bearing, moderately to well-sorted, locally well-stratified volcanic sand, gravelly sand, sandy gravel, and cobble gravel with minor silt (unit Qoa).

The clayey lahar deposit (unit Qvl) weathers to a dark yellowish brown (sub-weathering zone stratum not observed) and is mapped on the basis of one surface exposure and the occurrence of a soft clay-rich gravel (diamicton) layer stratigraphically interlayered with unit Qoa in the subsurface (Plate 3, cross sections A and B).

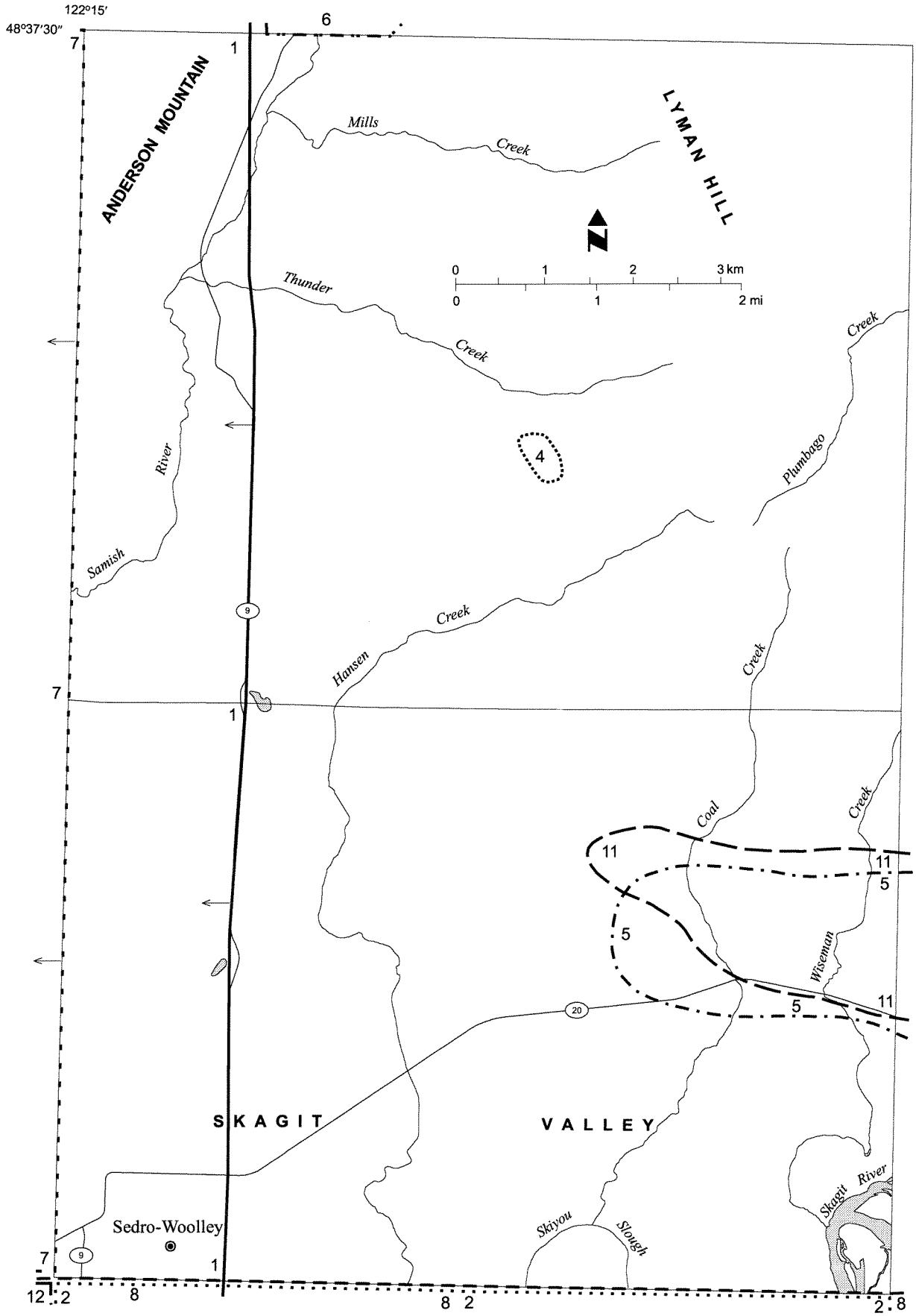

Figure 3. Location of previous geologic map studies in and adjacent to the Sedro-Woolley North *(this page)* and Lyman *(next page)* quadrangles. Study numbers are located inside the previous study area boundary. **1**, Dragovich and Grisamer (1998), 1:24,000; **2**, Whetten and others (1980a), 1:24,000; **3**, Whetten and others (1979), 1:24,000; **4**, Gallagher (1986) and Gallagher and others (1988), ~1:12,000; **5**, Heller (1978), 1:63,500; **6**, Kovanen (1996), 1:24,000; **7**, Dragovich and others (1998), 1:24,000; **8**, Pessl and others (1989) and Whetten and others (1988), 1:100,000;

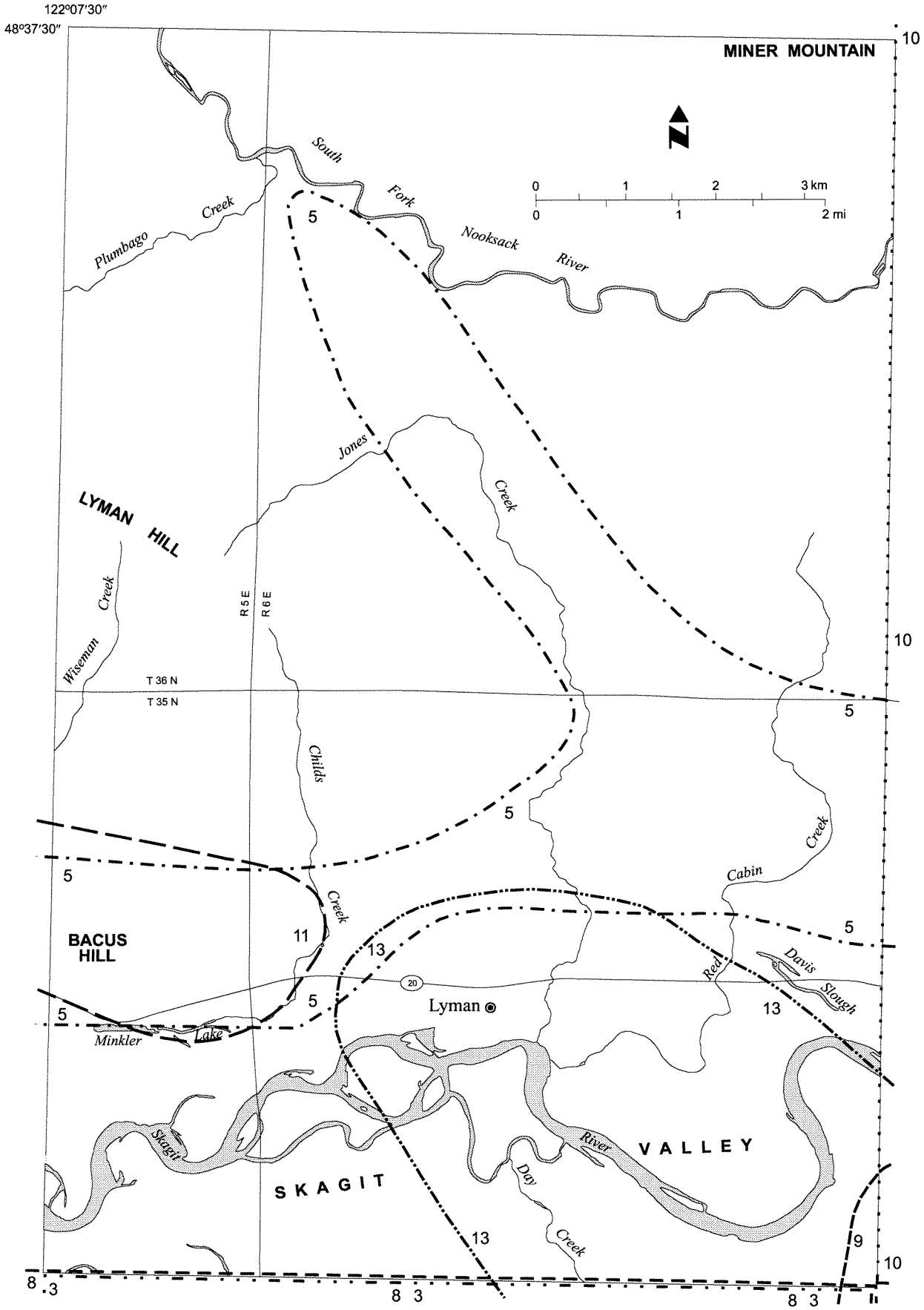

9, Robertson (1981), 1:20,000; **10**, Tabor and others (1994), 1:100,000; **11**, Jenkins (1924), 1:63,500; **12**, Dethier and Whetten (1981), 1:24,000; **13**, Foxall (1976), gravity study. Other important topical or regional studies include a 1:250,000-scale geologic compilation of the Helena–Haystack mélange and adjacent units by Tabor (1994), the 1:24,000-scale soil survey of Skagit County (Klungland and McArthur, 1989), and 1;24,000 Sumas outwash geologic mapping in the Samish River valley by Easterbrook (1979).

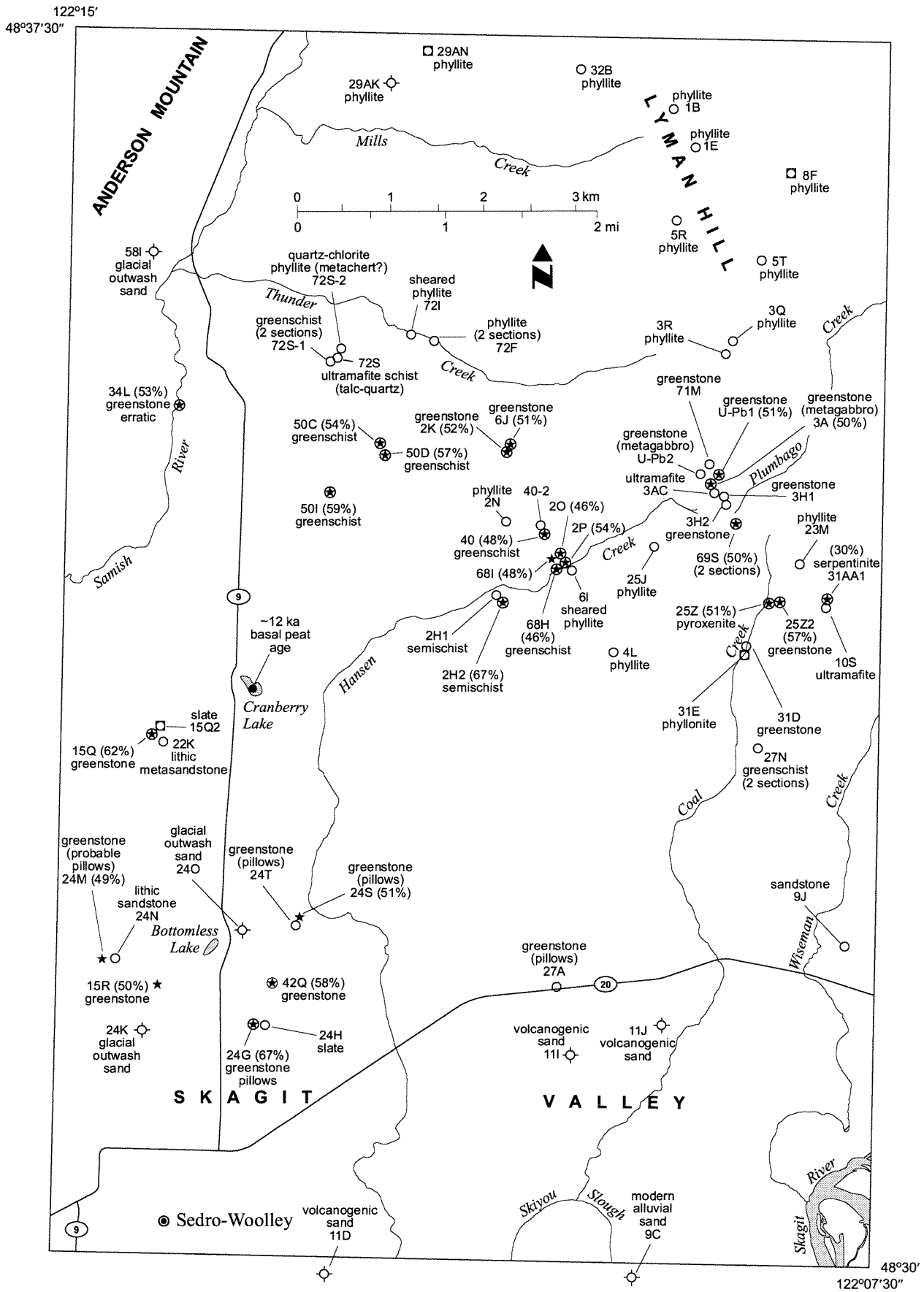

Figure 4. Sample site locations in and adjacent to the Sedro-Woolley North (*this page*) and Lyman (*next page*) quadrangles. Symbol explanation on page 8. Also see Figure 6 (this study) and plate 1 in Dragovich and others (in press b) for sample locations on portions of the Hamilton and Acme

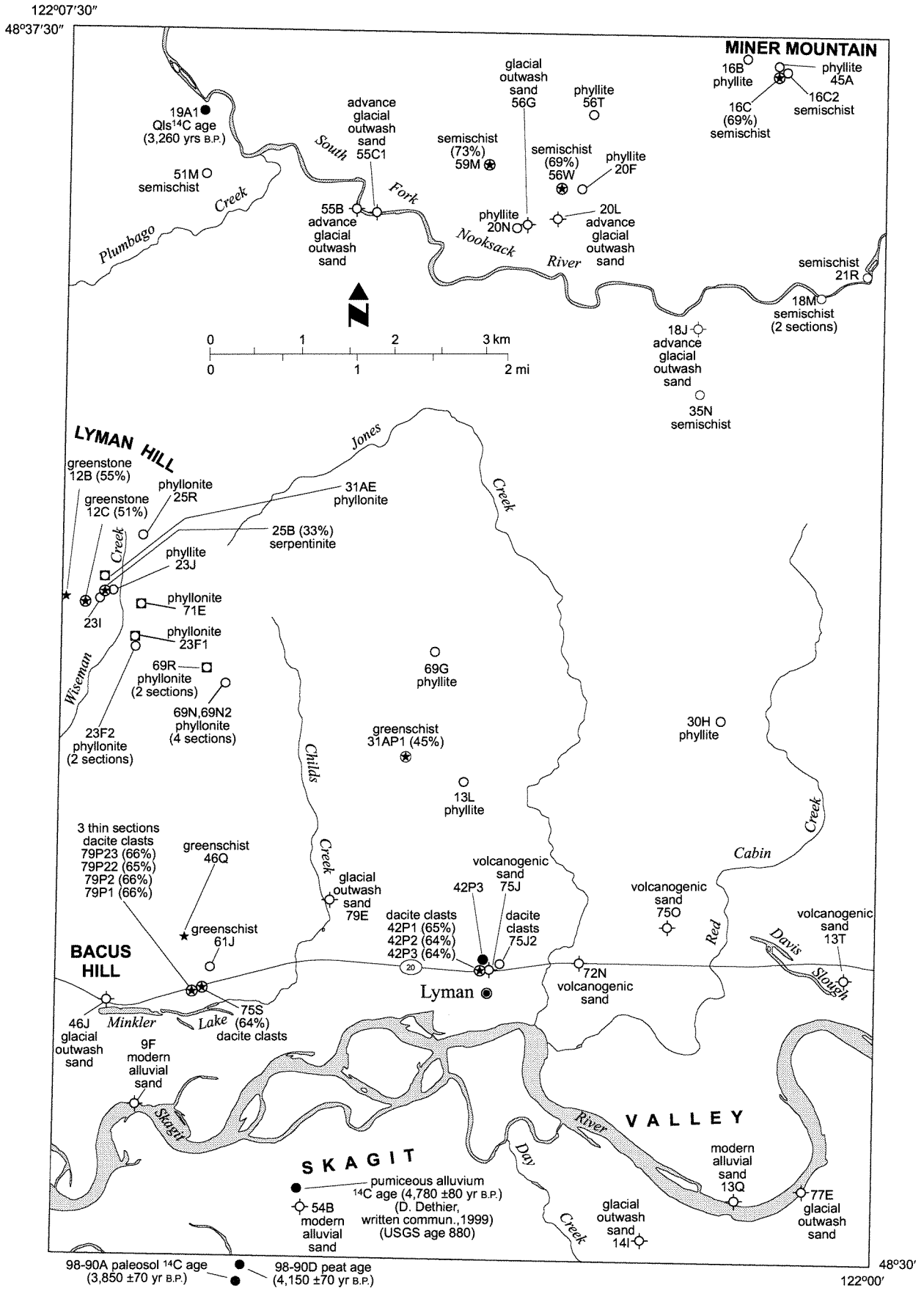

quadrangles directly adjacent to the primary Sedro-Woolley North and Lyman study area. Note the location of the USGS published and unpublished ^{14}C ages discussed in the text.

Unit Qoa volcaniclastic sands are brown to gray, depending on oxidation state and composition andare typically nonbedded to moderately well-bedded. Pumiceous microlitic volcanic-rich sand has a coarse 'flour' appearance in outcrop and is light olive gray and pale yellowish brown where weathered. Locally, unit Qoa terrace is mantled by laminated to massive overbank fine sand and silt.

Unit Qoa sand and gravel contain fresh vesicular dacite clasts and dacitic pumice derived from a Glacier Peak lahar(s) (Beget, 1982; Dethier and Whetten, 1981; Dragovich and others, 1998; D. Dethier, Williams College, written commun., 1999). Gravel-sized clasts in the lahar and volcaniclastic sandy gravel deposits in and around Lyman consist of chemically and petrographically distinct very light gray dacite clasts (Fig. 4)(appendices 1 and 2 of Dragovich and others, in press b). The units Qoa and Qvl contain less abundant clasts of phyllite, slate, and vein quartz with lesser miscellaneous clasts from bedrock and glacial deposits to the east.

We tentatively interpret unit Qoa to be the result of the attenuation of large noncohesive lahars at about 5,100 to 5,500 yr B.P. and possibly again at about 1,800 ^{14}C yr B.P. (Dragovich and others, in press a). At a depth of about 30 to 50 ft, unit Qoa overlies probable nonvolcanogenic alluvium and (or) late glacial deposits (Plate 3, cross sections A and B).

Qp **Peat (Holocene)**—Poorly stratified to unstratified, brown to black, fibrous to woody peat and muck of bogs and swamps in abandoned channels, kettles, and shallow oxbow lakes or depressions (for example, Minkler Lake in the Lyman quadrangle). Basal peat of Cranberry Lake (Plate 1) yielded a ^{14}C age of 12,900 ±500 yr B.P. (Rigg, 1958; Rubin and Alexander, 1958).

Qaf **Alluvial fan deposits (Holocene–latest Pleistocene)**—Poorly sorted to locally stratified diamicton consisting of clayey silty sandy gravel and gravelly sandy silt with angular to rounded clasts, mostly of debris-flow or debris-torrent origin and locally modified by stream processes. Clast composition reflects a local source area. Deposit thickness may locally exceed 60 ft. Unit Qaf disconformably overlies glacial deposits and disconformably overlies or interfingers with alluvium (units Qa, Qa_s, and Qa_{sf}) and thus is mostly Holocene (Plates 3 and 4). However, portions of the alluvial fans could be latest Pleistocene in age—the stratigraphically lowest portions of the largest alluvial fan complexes (for example, around the lower portion of Thunder Creek) may have initiated during deglaciation.

Qls **Landslide deposits, undivided (Holocene–Pleistocene)**—Poorly sorted, unstratified diamicton consisting of angular to rounded boulders, cobbles, and gravel in a sand, silt, and (or) clay matrix. Clast composition reflects local source area. Unit Qls includes deep-seated failures (slump-earthflow, debris slump, or rock slump) and, rarely, rock avalanche, fall, topple, and slab failures. Deep-seated landslides are locally associated with younger and smaller, superimposed debris flows and slides that emanate from unstable portions of the deep-seated landslide scarp, flanks, body, or toe. Although their thickness varies greatly, deep-seated landslide deposits are typically about 30 ft thick. They unconformably overlie bedrock and other Quaternary geologic units.

Landslides generally overlie late glacial deposits and thus are mostly Holocene. We obtained a ^{14}C age of 3,260 ±70 yr B.P. from the mid-outer rings of a barkless log surrounded by landslide debris in a cut-bank of the South Fork Nooksack River (Fig. 4). The log closely dates or provides a maximum age for the landslide deposit. The general lack of direct dates and the probability that unvegetated and locally steep slopes of unconsolidated glacial deposits were exposed during Everson deglaciation suggest that some of the landslide deposits may have been initiated in the late Pleistocene and may interfinger with late glacial materials at depth. Thus, thicker deposits are likely the result of slope instability and mass wasting during and after deglaciation. See Heller (1981) or Heller and Dethier (1981) for a discussion of the landslide types and controls in the lower Skagit River area.

GLACIAL DEPOSITS

Glacial deposits, from youngest to oldest, are divided into the Sumas Stade, Everson Interstade, Vashon Stade, and Evans Creek (alpine) Stade (Armstrong and others, 1965).

Deposits of the Fraser Glaciation, Sumas Stade

(Low-density deposits generally described as loose or soft)

Qgo_s **Glaciofluvial outwash (Pleistocene)**—Loose, moderately to well-sorted, subrounded to rounded cobbly sandy gravel, locally with boulders, sandy gravel, and minor gravelly medium to coarse sand, rare sandy silt, and silt; typically brown to gray, depending on oxidation state. Massive or moderately to well-bedded; crudely bedded on a scale of centimeters to, more commonly, a few meters as defined by clast size; locally contains lenticular interbeds of sand and (or) rare silty sand or silt. Mostly crudely subhorizontally stratified gravels with localized plane-bedded sand; rarely contains cross-stratified beds (few meters-thick sets); sediment transport downvalley or south to southwest to west. Directly west of the study area, gravel clast composition of the unit includes Twin Sisters Dunite (~15%), Mount Baker andesite (0–5%), and phyllite and vein quartz of Darrington Phyllite origin (0–15%)(Dragovich and others, 1998). Unit thickness in the study area is 10 to 50 ft (Plate 3, cross section D; Plate 4, cross section F).

EXPLANATION

- ⊹ Mounted sand thin section
- ○ Rock sample(s) for petrographic analysis (1 or more thin sections)
- ● Wood or shell ^{14}C sample site (this study)
- □ Ar-Ar muscovite age dating in progress
- ★ Geochemical analysis sample (% SiO_2 in parentheses adjacent to sample number)
- ⊛ Both geochemical and petrographic analysis sample (% SiO_2 in parentheses adjacent to samples analyzed for geochemistry)

Depositional environments for the Sumas deposits range from braided streams in the northwestern portion of the Sedro-Woolley North quadrangle to marine deltas at the junction of the Skagit valley and Sumas outwash valley train deposits in the Alger quadrangle west of the study area (Easterbrook, 1979; Dragovich and Grisamer, 1998) (Fig. 1). The latest Pleistocene lower Skagit valley appears to have been a marine embayment whose margin shifted as the crust rebounded from the Vashon Stade ice load. Sumas-time sea level is approximated by the altitude of the Sumas deltaic topset beds (now about 100 ft above present sea level) at the juncture of the Samish River with the Skagit River valley (Easterbrook, 1979).

Sumas outwash overlies older glacial deposits (Dragovich and others, 1997a,b,c; Dragovich and others, 1998; Dragovich and Grisamer, 1998). Deposition of Sumas outwash on Everson beach strand lines (Easterbrook, 1979) as well as boulder-size rip-up clasts of clay or clayey diamicton derived from underlying Fraser-age glaciomarine drift or till in the outwash best demonstrate the relative ages of unit Qgo_s and the older glacial deposits. The end of the Sumas Stade is approximately dated by ^{14}C methods at about 10,000 years (lowermost stratum of peat in abandoned Sumas outwash channels north of the study area; Easterbrook, 1962, 1969, 1971, 1976a,b). Wood from Sumas till in southwestern British Columbia yields more direct ^{14}C ages of 11,600 ±280, 11,500 ±1,100, 11,400 ±170, and 11,300 ±100 yr B.P. (Armstrong and others, 1965; Armstrong, 1981; Clague, 1980, 1981). Similarly, Clague and others (1998) report wood ages of 11,800 to 11,300 ^{14}C years for the Sumas deposits.

Deposits of the Fraser Glaciation, Everson Interstade

(Low-density deposits generally described as loose or soft)

The period of ablation of the Puget lobe during the Fraser Glaciation is termed the Everson Interstade. Ice removal and related isostatic rebound of the crust raised these deposits relative to their original depositional altitude during and immediately after the Everson Interstade. Significant glacial rebound occurred prior to Sumas Stade glacial re-advance into Whatcom County north of the study area. Everson Interstade deposits are overlain by Sumas outwash and unconformably overlie Vashon till and less commonly overlie older Quaternary deposits and bedrock (Plate 3, cross sections A–C, Fig. 3.1; Plate 4, cross sections E–G). Everson outwash rarely eroded downsection and was deposited directly onto Vashon advance outwash.

Several recent detailed glaciomarine stratigraphic studies have emphasized the diverse nature of the Everson deposits (Dethier and others, 1995, 1996; Pessl and others, 1989; Croll, 1980; Balzarini, 1981, 1983; Carlstad, 1992; Domack, 1982, 1983, 1984; Dragovich and others, 1998; Dragovich and Grisamer, 1998). The varied depositional facies and stratigraphy are the result of a complex interplay of ice-marginal and ice-distal sedimentary environments. Sedimentary facies reflect ice-marginal, fluvial-alluvial fan, marine fan, beach, deltaic, and turbidite depositional settings, as well as more open-water marine and estuarine settings in which ice-rafted and suspended sediment constantly dropped to the basin floor.

Facies groups of the Everson are distinguished on the basis of sedimentary structures, textures, altitude relative to the glaciomarine limit, and internal stratigraphy. Everson sedimentary facies observed in the study area include (1) ice-proximal terrestrial to marine outwash facies (units $Qgom_e$, Qgo_e, $Qgod_e$, Qgt_e); (2) moderately ice-proximal to ice-distal glaciomarine facies (units $Qgdm_e$, $Qgdm_{ec}$, $Qgdm_{ed}$); and (3) ice-proximal recessional lake facies (unit Qgl_e). The ice-proximal to ice-distal fine-grained facies contains glaciomarine drift (GMD)(unit $Qgdm_e$) that includes undivided clayey diamicton and (or) clay. This unit is locally divided into clast-rich GMD (unit $Qgdm_{ed}$) or clay GMD (unit $Qgdm_{ec}$) with few or no dropstones. Everson glaciomarine deposits in the study area lack fossils. The ice-proximal facies include subaerial outwash deposited near or above the glaciomarine limit of 360 to 400 ft (unit Qgo_e)[1]. Some subaerial outwash deposits may be kettle and kame deposits. Glaciomarine outwash (unit $Qgom_e$) was deposited near or below the glaciomarine limit of 360 to 400 ft. Unit $Qgom_e$ is locally divided into deltaic marine outwash deposits (unit $Qgod_e$). We have also mapped ice-proximal flow till north of Sedro-Woolley (unit Qgt_e) (Plate 4, cross sections F and G) and glacial lake rhythmite deposits (unit Qgl_e) in the South Fork Nooksack River valley.

Receding Everson glacial ice stagnated on the bedrock promontory bordering the northern part of the study area and on the Haystack–Cultus Mountain area directly to the south. Glacial ice meltwater deposited terrestrial outwash deposits above the glaciomarine limit. Three-dimensional geometries of outwash bodies (Plates 1, 3, and 4, Figs. 3.1 and 4.1) and other evidence indicate that these deposits were laid down concurrently with marine deltaic and turbidite outwash deposits.

Dragovich and others (1998) obtained a radiocarbon date of 13,270 ±50 yr B.P. from shell fragments in glaciomarine gravelly clay exposed at an altitude of about 340 ft along a logging road on Burlington Hill west-southwest of the study area. Subtraction of the marine water reservoir effect (for example, Dethier and others, 1995) gives an approximate age of 12,470 ±50 yr B.P. and allows for a comparison of Everson ^{14}C shell ages with Everson ^{14}C ages of woody organics. Dragovich and others (1998) report three woody organic ages (from sticks) of about 11,900 to 11,600 ^{14}C yr B.P. from the uppermost parts of ice-proximal glaciomarine outwash *and* the base of the overlying peat. These dates provide late and minimum depositional ages, respectively, for this outwash. The outwash was deposited near the glaciomarine limit. (See ^{14}C 'Alger age' note on Fig. 4.1C on Plate 4.) In the Sedro-Woolley North quadrangle, a basal peat sample from Cranberry Lake was obtained by Rigg (1958). The elevation of this sample is about 320 ft, or about 40 ft below the glaciomarine limit north of Sedro-Woolley (Fig. 4; Plate 1; Plate 4, cross section F, note by well 198). This sample provides an important limiting ^{14}C age of 12,900 ±500 yr B.P. (Rigg, 1958; Rubin and Alexander, 1958) for Everson Interstade deposition. These ages are consistent with local and regional ages of the Everson Interstade GMD and related deposits from about 13,500 to 11,000 yrs B.P. (Dethier and others, 1995). These ages, combined with the altitude and stratigraphic relations of our ^{14}C ages and nearby limiting ^{14}C ages of Siegfried (1978), indicate maximum glaciomarine inundation or highest marine limit south of a stagnating ice front before about 2,900 ^{14}C yr B.P. Corrected shell and wood ages from the general area suggest that the Everson Interstade

[1] A maximum glaciomarine limit (mgl) is defined as the highest altitude of Everson Interstade marine sediments mapped in the study area. In the study area, the mgl is consistently about 360 ft to perhaps as high as 400 ft and defines the uppermost limit of glaciomarine diamicton or clays.

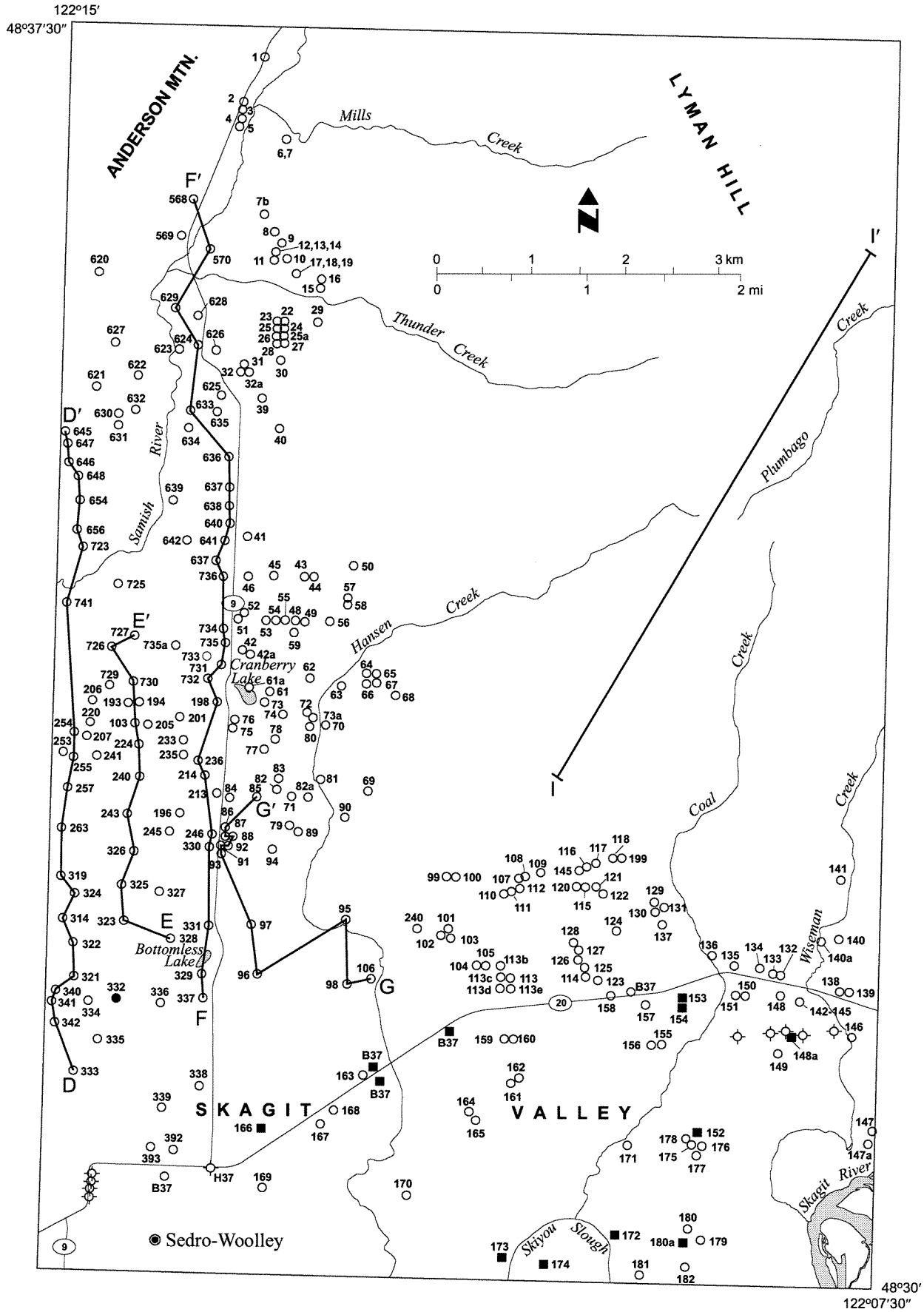

Figure 5. Location of selected water wells and geotechnical borings for the Sedro-Woolley North *(this page)* and Lyman *(next page)* quadrangles. We also analyzed, but do not show here, the logs of wells and borings within 1 to 2 mi of the north, south, and east borders of the study area. The

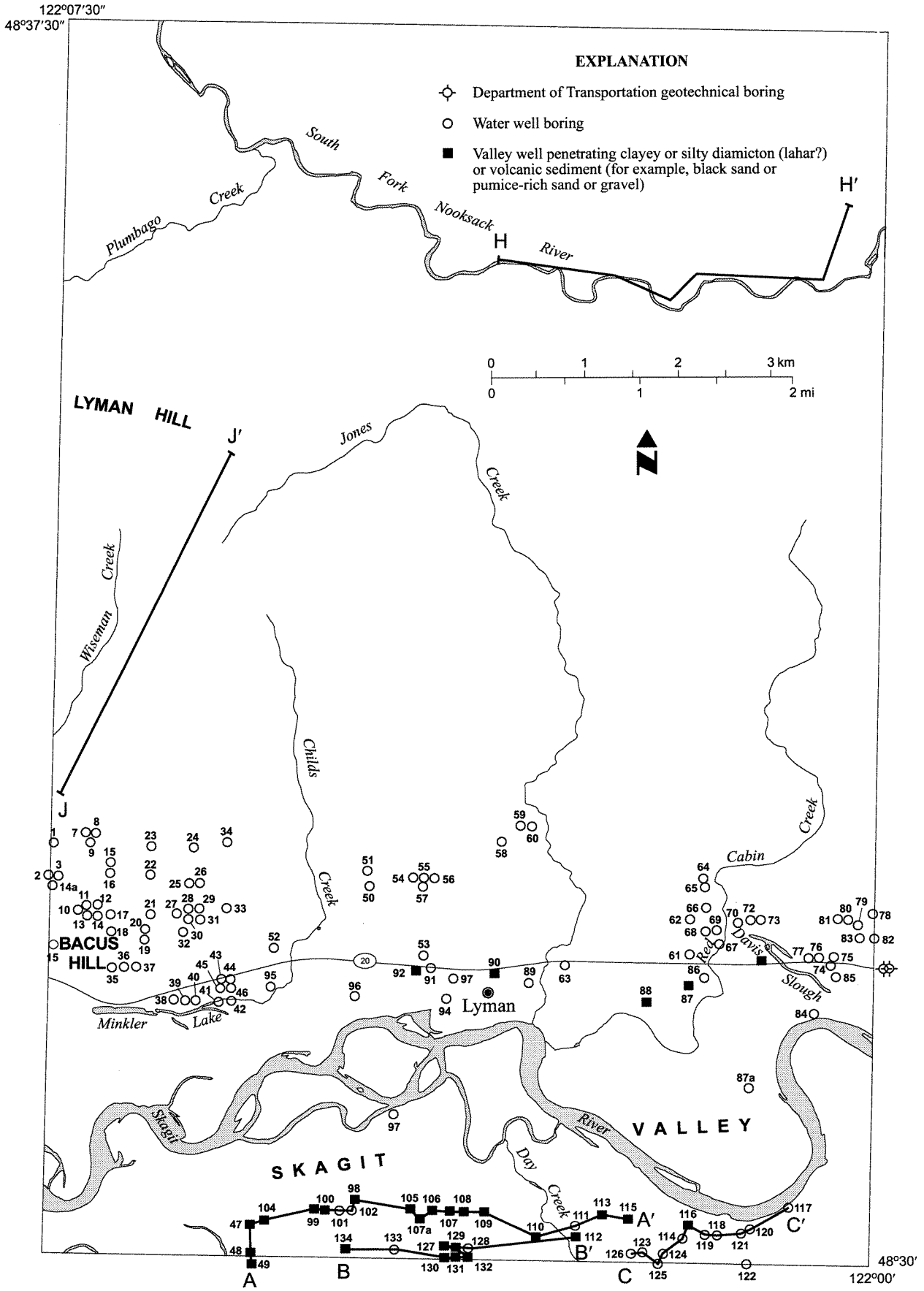

cross sections on Plates 3 and 4 show our interpretation of some of the water well data. Note the location of USGS published and unpublished ^{14}C ages discussed in the text.

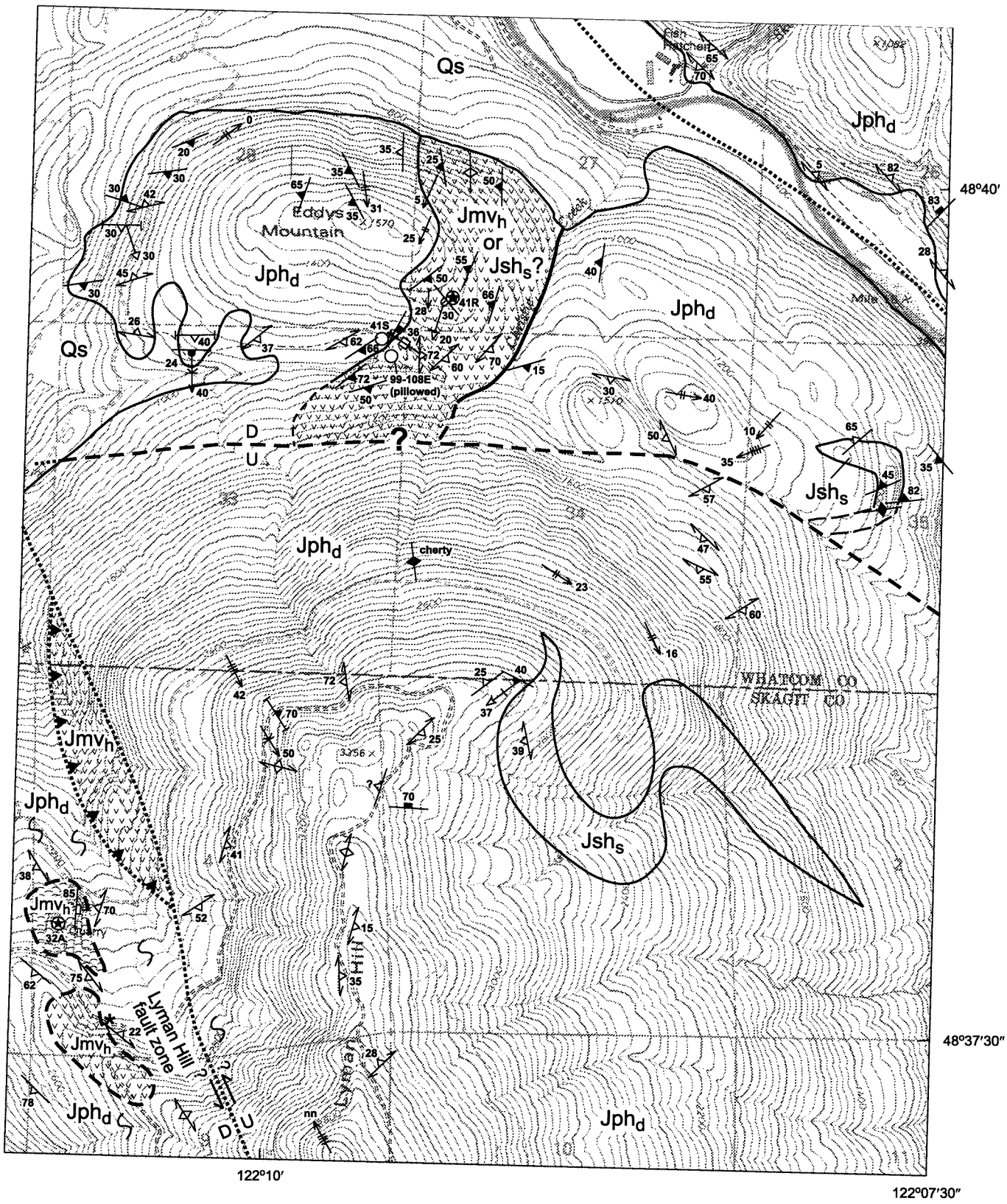

Figure 6. Geologic map of the south-central portion of the Acme 7.5 minute quadrangle. This quadrangle is directly north of the Sedro-Woolley North quadrangle. See Figure 4 for an explanation of the sample site symbols. Geologic explanation on facing page. Poorly recrystallized greenstones and serpentinite occur along the projection of the Lyman Hill fault zone (LHFZ) along the southwestern portion of the map. The greenstone blocks contain Fe-poor pumpellyite and fine-grained static metamorphic minerals. A north-northwest-striking cataclastic fabric and fracture cleavage of Tertiary(?) age is coincident with the LHFZ and projects under the Quaternary deposits of the broad Nooksack River valley. The mapped metabasaltic greenstone klippe on Eddys Mountain is underlain by phyllites and phyllonites locally containing a gently south-dipping penetrative S2 slaty cleavage that we correlate with mid-Cretaceous terrane stacking. The east–west-striking fault south of Eddys Mountain is suggested by a rarely observed fracture cleavage parallel to distinct lineament as seen in aerial photographs. The trend of this fault is subparallel to other mapped dip-slip or extensional faults in the area, such as the Coal Creek fault in the main study area.

marine and outwash deposits are about 12,900 to 11,600 ^{14}C yrs old (Dethier and others, 1995; Easterbrook, 1962, 1963, 1992; Armstrong and others, 1965; Dragovich and others, 1998). The abundance of local rock types as well as the position of unit Qgo_e at high elevations suggest a 'warm' basal ice erosion of nearby bedrock highlands. The composite Everson thickness ranges from a few feet up to 250 ft. (See Dragovich and others, in press b, for further discussion.)

$Qgdm_e$, $Qgdm_{ec}$, $Qgdm_{ed}$ **Glaciomarine drift (GMD), ice-proximal to ice-distal marine facies (Pleistocene)**—Poorly sorted, poorly compacted (soft when moist to rarely stiff) diamicton consisting of silty, sandy, gravelly clay to clayey gravel (unit $Qgdm_{ed}$); moderately well- to well-sorted sandy silt, sandy clay, clayey silt, and clay that lacks or contains only rare gravel, cobble, or boulder dropstones (unit $Qgdm_{ec}$). Undivided GMD (unit $Qgdm_e$) includes unit $Qgdm_{ec}$ silts and (or) clays and (or) unit $Qgdm_{ed}$ diamictons that are intimately interlayered or are not separated due to lack of information; diamictons are typically massive or contain very thick, crudely layered beds defined by varying gravel dropstone content; occasional latent vertical jointing; silts and clays are massive, or less commonly, varved or laminated rhythmites. GMD is brown to blue-gray to gray-blue; composite facies thickness is about 10 to 250 ft. Glaciomarine clays are locally 100 to 130+ ft thick (Plate 3, cross section D; Plate 4, cross sections E–G). These glaciomarine clays define the uppermost part of an overall upward-fining Everson glaciomarine stratigraphic sequence common in the lower Skagit River valley. (See Dragovich and others, 1998, in press b.)

We map Heller's (1978) glacial *lake* clays and dropstone-bearing diamictons directly north of the city of Lyman as Everson *glaciomarine* drift. Heller indicates that "the deposit is probably not glaciomarine as determined by the absence of macro-fossils, the limited extent of the deposit and its high elevation, above the reported elevations of GMD in the adjacent Puget Lowland." However, our more recent data and observations indicate that the GMD near the mountainous highlands characteristically lacks macrofossils. We mapped these deposits as Everson glaciomarine drift due to the low density of the deposits, stratigraphic position, and localized interlayering with phyllite-clast-rich Everson outwash, as well as their position relative to the Everson glaciomarine limit. The deposits in question occur near Lyman directly below the glaciomarine limit of 360 to 400 ft. (See Dragovich and others, in press b, for further discussion.)

Qgo_e, $Qgom_e$, $Qgod_e$, Qgt_e **Ice-proximal terrestrial to glaciomarine outwash facies (Pleistocene)**—Terrestrial recessional outwash (unit Qgo_e) consists of angular to subrounded phyllite- and vein-quartz-rich sand, sandy gravel, gravelly sand, and sandy cobbly gravel with rare interlayered thin to very thin beds of sandy silt and silt. Sands are typically light olive gray when dried and dusky yellow when weathered. The unit displays local low-amplitude foreset or trough cross-bedding, but more commonly displays crudely defined, approximately meter-thick subhorizontal beds defined by variations in cobble, gravel, and sand content. Beds commonly display a distinct pebble imbrication with internal truncation surfaces (scoured bedding) and a planar, low-amplitude foreset bedding indicative of a fluvial braided-channel environment. Subaerial or nonmarine outwash is mapped in the uplands (for example, Lyman Pass) and locally grades to topset beds of the deltaic outwash facies (unit $Qgod_e$) or undivided glaciomarine outwash (unit $Qgom_e$). North of Sedro-Woolley, foreset beds (~3 ft high) in terrestrial (nonmarine) outwash are locally steep (40–80°). This oversteepened bedding, along with probable kettles (with kames?) surrounded by outwash, as well as the spatial association with flow tills (see unit Qgt_e), indicate that grounded ice near the glaciomarine limit has deformed these ice-proximal glacial sediments via ice shove or ice collapse.

Undivided glaciomarine outwash (unit $Qgom_e$) consists of subangular to subrounded to locally angular sandy gravel, gravelly sand, and silty sand with lesser sandy cobbly gravel with interlayered silt beds. Typically brown to gray in color; commonly thickly to thinly bedded, rarely nonbedded or massive. Bedding varies from distinctly plane-laminated to horizontally stratified with crudely bedded sands and gravels; soft-sediment deformation structures and steep bedding are rare. Unit $Qgom_e$ occurs below the glaciomarine limit of 360 to 400 ft. More distal glaciomarine outwash is thinly laminated to varved (silt to sandy silt or silty sand couplets) similar to rhythmi-

EXPLANATION

Geologic Units

SEDIMENTARY DEPOSITS

Quaternary sedimentary deposits

Qs Surficial deposits, undivided

LOW-GRADE LAYERED METAMORPHIC ROCKS OF THE NORTHWEST CASCADE SYSTEM

Mesozoic metamorphic rocks of the Shuksan nappe of Tabor and others (1994)

Easton metamorphic suite of Misch (1966) (Jurassic)

Jph_d Darrington Phyllite (0–10% interlayered semischistose metasandstone)

Jsh_s Shuksan Greenschist

Mesozoic metamorphic rocks of the Haystack thrust nappe of Whetten and others (1988) and the Helena–Haystack mélange of Tabor (1994) (Jurassic)

Generally, blocks in a serpentinite-matrix mélange overlying the Easton Metamorphic Suite in the study area

Jmv_h Metabasalt

pillow metabasalts metabasalts

★ Serpentinite pods and outcroppings too small to show at map scale

Geologic Map Symbols

Contact – Dashed where inferred; dotted where concealed

High-angle fault – Dashed where inferred; dotted where concealed; U, upthrown block; D, downthrown block; half arrows indicate relative apparent strike-slip motion

Thrust fault – Dashed where inferred; dotted where concealed; sawteeth on upper plate

See Plate 2 for an explanation of foliation and lineation symbols

cally bedded glaciomarine outwash on Whidbey Island described by Domack (1984).

Everson Interstade outwash grades from sandy gravel and gravel to dominantly sand and silty sand. (See 'fining' symbol on Plates 1 and 2; Plate 3, cross section C; and Plate 4, cross section G.) Interbedded with the sand and gravel is clay or clayey diamict (unit $Qgdm_e$). This interlayering attests to cyclic deltaic-turbiditic deposition along a shifting delta or submarine fan front; that is, glaciomarine deposition from iceberg melting and marine suspended-load deposition interlayering with submarine outwash.

Flow(?) till (unit Qgt_e) typically consists of clayey, silty, sandy gravel diamicton to silty, sandy, gravel with boulder diamicton; massive; small outcrops occur north of Sedro-Woolley and are near the glaciomarine limit of 360 to 400 ft where liquefied till was deposited onto the adjacent outwash plain. A subtle and localized east–west-trending microtopography (~20-ft high linear ridges) north of Sedro-Woolley is suggestive of modified morainal washboard ridges composed mostly of interlayered outwash, flow till, and locally overlying marine clays.

Deltaic deposits (unit $Qgod_e$) consist of sand and sandy gravel, locally with some cobbles; typically thinly to thickly bedded on a scale of centimeters to a few meters; very commonly display planar high-amplitude foreset beds indicative of deltaic deposition; foresets are at least tens of meters high and dip 15 to 40° (avg. ~32°) toward the Skagit River embayment; foresets are locally overlain along a distinct truncation surface by 3 to 7 ft of sandy cobbly gravel suggestive of topset beds. Subhorizontal topset beds of nonmarine outwash (unit Qgo_e) appear as crudely bedded gravels with interbeds of sand and (or) rare silty sand or silt. Bottomset beds of glaciomarine clay and clayey diamicton are composed of massive to laminated silty clay and clay. We have traced outwash above the glaciomarine limit to deltaic deposits near the glaciomarine limit to glaciomarine clay with minor localized dropstones below the glaciomarine limit (For example, Fig. 4, near site 14I; Plate 3, cross section C).

Qgl_e **Recessional glacial lake rhythmites of the South Fork Nooksack River and Lyman Hill**—Consists of soft to stiff silty clay, clayey silt, silty sand, and sand with local dropstones; moderately to well-sorted, rhythmically bedded and (or) varved; rhythmite bedding typically about 1 cm thick, coarsening upward from silty clay to silty sand or sand; included in this unit are glacial lake sediments high on Lyman Hill that consist of varved to laminated sandy silt or clayey silt-sand rhythmites with soft-sediment deformational features (tilted, folded, or contorted bedding) suggestive of ice buttress collapse. These low-density, glaciolacustrine deposits probably formed in temporary glacial lakes impounded by retreating glacial ice and topographic barriers (for example, Lyman Hill and Miner Mountain).

Deposits of the Fraser Glaciation, Vashon Stade

(Moderate- to high-density deposits generally described as compact or hard or stiff)

Qgt_v **Till (Pleistocene)**—Nonstratified, dense to very dense diamicton consisting of clay, silt, sand, and gravel in various proportions, with scattered cobbles and boulders; rare lenses of sand or gravel indicate subglacial meltwater processes were active during deposition; dark yellowish brown to brownish gray; clast derivation from the Coast Plutonic Complex of British Columbia (for example, Easterbrook, 1962); commonly contains abundant phyllite or local bedrock clasts; ranges from a few feet to locally up to about 80 ft thick.

Till unconformably overlies bedrock and advance outwash and, much less commonly, older glacial units (Plate 3, cross section C). Very commonly underlies glaciomarine drift below the glaciomarine limit of 360 to 400 ft. (For criteria to differentiate till and glaciomarine drift, see Dragovich and others, 1998; Dragovich and Grisamer, 1998; or Easterbrook, 1962.) Till is locally overlain by a few meters of ablation till indicative of ice stagnation on the upland and mountainous areas. (Also see Heller, 1978.)

Radiocarbon dates from other areas indicate an age between 18,000 and 13,600 yr B.P.

Qga_v **Advance outwash (Pleistocene)**—Moderately to well-sorted, stratified, highly compacted medium to coarse sand, pebbly sand, and sandy gravel, with minor amounts of fine silty sand or sandy silt, and clay interbeds with scattered lenses and layers of pebble-cobble gravel; medium gray when dried; weathers to a pale yellowish brown; thinly to very thickly bedded with subhorizontal bedding or generally south-dipping cross-stratification; localized cut and fill structures, less commonly trough or ripple cross-bedded. Local high-amplitude foreset bedding suggests deltaic deposition into proglacial lakes; thickness ranges from 20 to 100+ ft.

The unit commonly forms an overall coarsening-upward sequence from sand, silt, and clay at the base (noted only in well logs) to sand and gravel with locally cobbly gravels at the top (Dragovich and Grisamer, 1998). Advance outwash buries a more dissected pre-Fraser intraglacial topography (Plate 3, cross section C, Fig. 3.1).

As also observed south of the study area by Pessl and others (1989), sand and gravel advance outwash overlies 'transitional beds' consisting of undifferentiated early Vashon advance outwash and (or) late pre-Vashon nonglacial deposits. We tentatively equate clays containing scattered gravel observed in the subsurface of the Skagit River valley (Plate 3, cross section C) with advance lake deposits. Lake deposits may underlie advance outwash deposits as a result of glacial lake impoundment during ice advance up the Skagit River valley (Heller, 1978). This is similar to glacial advance lake deposits in the South Fork Nooksack River as described below.

Qgl_v **Advance glacial lake rhythmites and associated glacial outwash sediments of the South Fork Nooksack River (Pleistocene)**—Consists of very thinly to thickly bedded clay, clayey silt, silt, and silty sand with local dropstones; also includes interlayers of sand, sandy gravel, and cobbly gravel, as well as rare, typically clast-supported, boulder gravel deposits with a little sandy silt matrix of both flow till and valley-

margin alluvial fan origin. Sand lenses are common in silt and gravel layers; silts gray to brown; sands various shades of gray when dried and pale yellowish brown when weathered; rhythmite (varve?) bedding typically 1 cm thick, coarsening upward from silty clay to silty sand or sand; elsewhere rhythmic bedding is less pronounced and the interlayered clays, silts, and sands, with lesser interlayered gravels, are well-stratified and thinly to thickly bedded; gravel and massive silt layers commonly contain rip-up clasts of glacial lake rhythmites; soft-sediment deformational features are pervasive in silts and clays and include contorted bedding, overturned folds, ice-shove faults, and rarely flame structures (Plate 1); sands commonly plane-bedded; thickness varies from 20 to 100 ft.

Glacial lake sediments (unit Qgl_v) in the valley bottom of the South Fork Nooksack River generally grade upward to advance outwash (unit Qga_v) (Plate 4, cross section H). Units Qgl_v and Qga_v are interlayered on a scale of a few inches to as much as tens of feet and define an overall coarsening-upward sequence. We mapped areas with more than 50 percent interlayered outwash sand and gravel as unit Qga_v; gravel and sand clast compositions indicate a mixed provenance of nearby North Cascades and far-traveled Canadian origin. (See Dragovich and others, in press b, for sand compositional data.) Lake sediments and (or) related advance outwash are locally overlain by Vashon till and overlie a dense till 'river pavement' along the South Fork Nooksack River. We correlate the river pavement till with the Evans Creek (alpine) Stade till as described below. (See Plate 4, cross section H.)

Deposits of the Fraser Glaciation, Evans Creek Stade

(Moderate- to high-density deposits generally described as compact or stiff)

Qat_{ec} **Till (Pleistocene)**—Typically massive, clayey, silty, sandy gravel diamicton; clast types indicate local eastern, or upvalley of the South Fork Nooksack River, provenance (clasts mostly dunite, pyroxenite, slate, phyllite, volcanic, and metavolcanic clasts). Occurs at several localities as a very dense 'river pavement' near and below low-water level of the South Fork Nooksack River. Unit is overlain by advance lake sediments and locally by advance outwash (units Qgl_v and Qga_v, respectively) and is inferred to be underlain by bedrock. Similar tills occur on the mid- to lower slopes of Miner Mountain, north of the Nooksack River. These till outcrops contain cobble and gravel clasts of dunite (~43%), pyroxenite (~30%), peridotite (~3%), vein quartz (~7%), phyllite (~5%), semischist (~5%), metasiltstone and slate (~3%), and chert or metachert (~3%). We tentatively correlate these elevated tills with the Nooksack River pavement tills. These tills may also correlate with till exposed in an escarpment (under advance outwash) near the city of Lyman (Heller, 1978). We cannot exclude the possibility that the Miner Mountain dunite-rich till outcroppings are the Sumas Stade (alpine) advance tills of Kovanen (1996). (See Dragovich and others, in press b, for further discussion.)

Tertiary Sedimentary Rocks

Ec_{cb} **Bellingham Bay Member of the Chuckanut Formation (Eocene)**—Very light gray feldspathic sandstone (arkose); clasts consist dominantly of monocrystalline quartz, plagioclase, potassium feldspar, and biotite, with lesser muscovite and lithic fragments (phyllite) and polycrystalline quartz and chert; also includes detrital chlorite and sphene (this study; Johnson, 1982). Accessories include opaque minerals and zircon (Johnson, 1982, 1984). Thickly to very thinly bedded, well-sorted, rounded to subrounded, medium- to coarse-grained, micaceous feldspathic sandstone and minor polymictic conglomerate (coarse-grained intervals) alternating with abundant mudstone and lesser fine-grained feldspathic sandstone, siltstone, and minor coal (fine-grained intervals). The contact between the Chuckanut Formation and the Darrington Phyllite in the southeast corner of the Lyman quadrangle is mapped as a high-angle, northwest-trending fault that we informally name the Coal Creek fault.

Regionally, Johnson (1982, 1984) divided the Chuckanut Formation into the Bellingham Bay and Slide Mountain Members. Johnson also named the Padden, Maple Falls, and Governors Point Members of the informally named upper Chuckanut Formation. The Bellingham Bay Member of Johnson is equivalent to the Coal Mountain unit of Evans and Ristow (1994). Mustoe and Gannaway (1997) and Dragovich and others (1997b) include the Bellingham Bay and Slide Members in the informally named lower Chuckanut Formation. Mustoe and Gannaway (1997) examined the flora of the Chuckanut Formation and proposed an Oligocene age for the upper part of the formation. However, an Eocene age for most of the Chuckanut lithostratigraphic equivalents in western Washington and the central Cascades is consistent with the radiometric ages of interbedded volcanic rocks (Mustoe and Gannaway, 1997; Johnson, 1984; Johnson and others, 1983; Evans and Ristow, 1994; Reiswig, 1982). Near Mount Vernon, the Coal Mountain unit contains a tuff with a revised zircon fission-track age of 52.6 ±4.8 Ma (R. W. Tabor, USGS, written commun. to Evans and Ristow, 1994), and the Coal Mountain unit is cut by a variety of dikes with ages ranging from 41 to 50 Ma (Whetten and others, 1988).

Paleocurrent, fission-track, and provenance data suggest that the potassium-feldspar-rich feldspathic arkosic sandstones of the lower Chuckanut Formation were derived from uplifted crystalline basement rocks east of the Crystalline Core (fig. 2 of Dragovich and others, in press b), possibly derived from the rapidly uplifted and eroded Omineca Crystalline Complex in north-central Washington (Johnson, 1982). Faulting, uplift, and erosion of locally derived basement detritus and transport into mostly fault-controlled fluvial basins are clearly documented for the younger Chuckanut Formation members (for example, Evans and Ristow, 1994; Mustoe and Gannaway, 1997). The occurrence of minor but significant foliate polycrystalline quartz aggregates (much of which is probable phyllite), phyllite, greenstone, greenschist, and serpentinite lithic clasts in arkoses of the Chuckanut Formation in and near the study area (this study; Robertson, 1981) indi-

cates basement exposure during deposition of the east-derived Bellingham Bay Member. Subaerial exposure of the basement is suggested by the local derivation of some of the arkoses of the Coal Mountain unit. This may be indicative of some basin instability and faulting, possibly along trends such as the Coal Creek fault, during deposition of the lower Chuckanut Formation in the study area.

Low-Grade Metamorphic Rocks of the Northwest Cascades System

We divide the pre-Tertiary rocks of the Northwest Cascades system (fig. 2 of Dragovich and others, in press b) in the study area into two structural units that are separated by a probable mid-Cretaceous thrust fault: (1) the Shuksan nappe, composed of the Easton metamorphic suite (Easton suite), and (2) the overlying Helena–Haystack mélange (HH) of Tabor (1994) or Haystack nappe of Whetten and others (1980b). Our thrust-bounded lithologic packages are largely consistent with Northwest Cascades system thrust stratigraphy of Tabor (1994)(fig. 5 of Dragovich and others, in press b) and Brown and others (1987)(Deer Peak unit shown in fig. 6 of Dragovich and others, in press b). Dragovich and others (1998) mapped the informally named Whitehall Creek thrust fault between the Shuksan and HH nappes on Chuckanut, Colony, and Blanchard mountains in the Bow quadrangle west of the study area (Fig. 1). In the present study area, we mapped similar greenstone-serpentinite-bearing klippen on top of Lyman Hill in the Sedro-Woolley North and Lyman 7.5-minute quadrangles. We also mapped a possible HH klippe on top of Mount Josephine in the Hamilton 7.5-minute quadrangle (plate 1 of Dragovich and others, in press b) directly adjacent to the primary study area.

Evidence for a thrust fault separating the HH and Shuksan nappes includes metamorphic as well as lithologic, geochemical, magnetic, and structural differences across the fault contact and the spatial association of the thrust-fault zone with alpine ultramafic bodies and post-peak metamorphic protomylonites and mylonites. We suggest that D2–D3 fabric elements (see below) of the Shuksan and HH are the result of an inhomogeneous simple shear affecting the nappes. (See Dragovich and others, 1998. Also plate 1, table 4, and figs. 7–10 of Dragovich and others, in press b, provide a map, tables, sketches, and stereonet data that illustrate our structural model for the HH and Easton suite.) Not all workers agree with our interpretation. Gallagher (1986) and Gallagher and others (1988) include some of the meta-igneous rocks (for example, some of the greenstones and ultramafite outcroppings on Lyman Hill) in the Easton metamorphic suite.

MESOZOIC METAMORPHIC ROCKS OF THE SHUKSAN NAPPE OF TABOR AND OTHERS (1994)

The Shuksan nappe (fig. 6 of Dragovich and others, in press b) is composed of the Easton metamorphic suite (Easton suite, herein). The Easton suite includes the Darrington Phyllite of Misch (1966) and metasedimentary and metavolcanic facies variants and corresponds to the Shuksan metamorphic suite of Misch (1966), Brown (1986, 1987), and Brown and others (1987). Regionally, the Easton suite of Tabor and others (1993, 1994) includes the Darrington Phyllite (unit Jph_d), the semischist of Mount Josephine (unit Jph_j), as well as the Shuksan Greenschist (unit Jsh_s). Manganese-rich pelitic protoliths common in the eastern part of the Easton suite belt mostly reflect deep-basin (locally cherty) sedimentation on mid-ocean ridge basaltic crust (Shuksan Greenschist protolith). Elsewhere, particularly in the western part of the Easton suite belt, areas rich in semischistose metasandstone with lesser metaconglomerate probably represent sedimentation near an island or continental arc. We suggest that the preserved bedding geometries and sedimentary structures of the metamorphosed sandstone, siltstone, shale, and rare conglomerate of the unit suggest turbidites of a submarine fan sequence near a volcanic arc. (See Dragovich and others, in press b, for further discussion.)

U-Pb, Rb-Sr , and various K-Ar age estimates for the Easton suite indicate a pre-Cretaceous or Late Jurassic protolith or depositional age. Armstrong (1980) and Brown and others (1982) proposed that the age of the oceanic protolith of the Easton suite was Jurassic, possibly Late Jurassic. A probable Middle Jurassic protolith age for the Easton is indicated by a zircon age of 163 Ma from diorite on Bowman Mountain, north of the Lyman quadrangle (Gallagher and others, 1988). Dragovich and others (1998) obtained a nearly concordant $^{206}Pb/^{238}U$ zircon age of 163.8 ±0.2 Ma and a $^{207}Pb/^{235}U$ zircon age of 164.0 ±0.2 Ma from a greenschist klippen on Anderson Mountain directly west of the Sedro-Woolley North quadrangle. Dragovich and others (1998) tentatively interpreted this rock to be a Shuksan Greenschist klippe in the HH mélange on Anderson Mountain. The age date supports a Jurassic protolith age for the Easton.

The Easton suite was metamorphosed to blueschist facies at about 110 to 130 Ma (Brown and others, 1982), possibly into the Late Jurassic (Armstrong and Misch, 1987) and after an early seafloor metamorphism or hydrothermal alteration event (Haugerud, 1980). The consequent degree of Easton suite recrystallization is consistent with geothermobarometric analyses (350–400°C, 7–9 kb) by Haugerud and others (1981), Brown and others (1981), and Brown (1986).

The first deformation (D1) fabric elements in the Easton suite include a distinct and pervasive first-generation foliation (S1), a first-generation lineation (L1) on the S1 surface, and rarely observed first-generation folds (F1) of the bedding. Easton suite rocks typically contain a granoblastic quartzose matrix with a distinct quartzose and micaceous (lepidoblastic) segregation layering (0.5–3 mm thick) along S1. The S1 fabric is syntectonic and is characterized by pervasive and strong metamorphic recrystallization. S1 parallels locally preserved bedding structures as a result of transposition of primary layering during syn-D1 blueschist-facies metamorphism. (See fig. 7 and table 4 of Dragovich and others, in press b.) S1 is crenulated one or, locally, two times as a result of second-generation (F2) and third-generation (F3) microfolding. At outcrop scale, semischist is typically characterized by a strong S1 planar cleavage, a strong L1 clast-stretching lineation, and a distinct L2 crenulation lineation defined by the F2 microfolds. The style of F2 folds in phyllitic metasiltstone or metashale interlayers (for example, megascopically folded) in the semischistose metasandstone (for example, microscopically crenulated) demonstrate that the style of folding is a reflection of the competency contrast between the metasedimentary units.

Texturally, greenschists are well to very well recrystallized and strongly S1 foliate. Greenschists are tabular to lensoidal-shaped and tens to a few hundreds of meters thick with a strong S1 foliation subparallel to their length. The greenschists are typically semicontinuous along strike, and where well exposed, are clearly interlayered with Easton semischist-phyllite sequence. The foliated metatuffaceous to metavolcanic flow units share the S1 foliation, L1 lineation, and locally, the L2 crenulation

lineation (F2 microfolds) with the adjacent metasedimentary units of the Easton suite.

Contacts between the Darrington and Mount Josephine subunits are gradational in the field and thus are represented by the mostly dashed contacts between these units. However, distinct primary textural changes occur across many Tertiary high-angle faults, where mostly phyllite with little semischistose metasandstone is exposed on one side of the fault and mostly semischistose metasandstone is exposed on the other side (Plate 1; Plate 4, cross section H).

Thrusting is inferred to have occurred in the mid-Cretaceous (88–100 Ma) during low-temperature blueschist facies metamorphism in the San Juans, but probably after blueschist metamorphism of the Easton suite in the Northwest Cascades system (Brandon and others, 1988; Brown, 1987). Tight folding of S1 cleavages is locally associated with an incipient to penetrative, spaced to slaty S2 foliation. Phyllites are D3 protomylonitized or mylonitized and F3 folded near the thrust contact with the overlying HH (mylonitized phyllites = phyllonites). (See Dragovich and others, in press b.)

Jph_d, Jph_{dj}, Jph_{jd}, Jph_j, Jsh_s **Easton Metamorphic Suite of Tabor and others (1993)(Jurassic)**—The Darrington Phyllite and semischist of Mount Josephine are not strictly separate rock units. Our separation of the Darrington Phyllite of Misch (1966) into fine-grained (Darrington) and coarse-grained (Mount Josephine) rock unit protoliths reflects our effort to map the proportions of phyllite and semischistose metasandstone in different parts of the study area. End-member metasedimentary compositions are metapelite (shale) to siliceous argillite (Darrington Phyllite), which grades to the metagraywacke and arkosic semischistose metasandstone of Mount Josephine with increasing relict sand and gravel content. Petrographic examination of our protolith classifications supported our field interpretation. The metasedimentary rocks of the suite are divided into:

- Jph_d Darrington Phyllite (<10% interlayered semischist)
- Jph_{dj} Darrington Phyllite (10–50% interlayered semischist)
- Jph_{jd} Semischist of Mount Josephine (10–50% interlayered phyllite)
- Jph_j Semischist of Mount Josephine (<10% interlayered phyllite)

We observed interlayered metapelite and metaargillite (Darrington) semischistose metasandstone and lesser metaconglomerate (Mount Josephine) at thin-section, outcrop, and mountain scales. We divided units on the basis of outcrop-scale proportions of metasandstone and phyllite. Prominent original grain-size variations from metasiltstone-metashale (phyllite) to metasandstone-metaconglomerate (semischist) occur on a scale of millimeters to a few meters. For example, semischist contains very thin to medium-bedded phyllitic interlayers and generally equigranular metasandstone and pebble conglomerate that locally display distinct grain-size variations reflecting crude to distinct primary graded bedding. Intercalations of phyllite in semischistose sandstone occur on a scale of millimeters to meters (typically centimeters) defining very thin to thick beds; rip-up clasts of phyllite (meta-argillite) occur in metasandstones and metaconglomerates and are typically larger than other clast types.

Jph_d, Jph_{dj} **Darrington Phyllite (Jurassic)**—Graphitic quartzose muscovite-chlorite phyllite or phyllonites with lesser calcareous graphitic quartzose phyllite (metamarl?) to micaceous quartzite (metachert?) with up to 50 percent interlayered metasandstone and rare metaconglomerate; typically strongly S1 foliate; phyllites are light gray to dark gray and weather to yellow-gray or light olive gray; metacherts are olive gray; finer grained protoliths are darker, mostly as a result of increased primary matrix organic material that reacted to form graphite during metamorphism. Dominant metamorphic minerals include polygonal granoblastic to slightly sutured quartz (20–69%, avg. 42%), muscovite (20–44%, avg. 32%), Mg-chlorite (0–22%, avg. 6%), Fe-chlorite (0–12%, avg. 6%), graphite (0–9%, avg. 3%), and epidote (0–5%, avg. 1%); other minerals include albite (0–15%, avg. 6%), calcite (0–3%), and rare Al-pumpellyite and lawsonite. (Pumpellyite, chlorite, and muscovite compositional data was determined using an electron microprobe [analyst Amy Johnson, USGS, unpub. data].) Accessory minerals include opaques (including pyrite), titanite (sphene), stilpnomelane, iron oxide, and very commonly, tourmaline. Relict clasts are mostly subangular, sand- to silt-size (typically 0.01–0.1mm in diameter but rarely may be as much as 0.5 mm in diameter) with monocrystalline and polycrystalline quartz and plagioclase constituting up to 25 modal percent of the sample in meta-argillaceous varieties of phyllite. Relict clasts were observed in about 40 percent of the phyllite samples. Other samples are completely recrystallized pelites or semipelites and exhibit no primary relict lithic clasts or minerals. Phyllonites contain similar mineralogy. However, grain reduction of the quartzose matrix in the phyllonites is prominent and muscovite content is somewhat increased by the grain reduction, recrystallization, and retrogressive breakdown of plagioclase relict clasts and matrix to form muscovite.

Jph_j, Jph_{jd} **Semischist of Mount Josephine (Jurassic)**—Semischistose arkosic to lithic arkosic sandstone or feldspathic metagraywacke and rare pebble metaconglomerate; up to 50 percent interlayered phyllite; strongly S1 foliate; typically light gray, medium gray, or dark gray, weathering to a pale yellow brown or green gray. Dominant metamorphic minerals include polygonal granoblastic quartz (0–44%, avg. 24%), albite (0–25%, avg. 9%), lepidoblastic muscovite (0–30%, avg. 17%), actinolite (0–5%, avg. 1%), Fe-chlorite (0–10%, avg. 4%), Mg-chlorite (0–15%, avg. 6%), stilpnomelane (0–5%, avg. 1%), and epidote (0–5%, avg. 2%). Other minerals are calcite (0–4%), and graphite (0–4%); accessory minerals include hornblende, opaques (including pyrite), titanite, iron oxide, and rarely tourmaline. Minor potassium feldspar is present in mylonitized rocks adjacent to Tertiary faults as a result of metamorphic retrogression during low-temperature shear deformation.

Stretched subrounded to subangular (rarely rounded) relict sand- (typically 0.05–2 mm in diame-

ter) to rarely pebble-size clasts, mostly include polycrystalline quartz (40–60%), monocrystalline quartz (5–30%), albite (5–60%), and graphitic to micaceous metamorphosed pelitic to semipelitic rip-up clasts (0–15%). Typically quartz and plagioclase relict grains are equal in abundance. Schmidt (1972) indicates that relict plagioclase grains are mostly decalcified (An_{4-6}) and locally sericitized in the phyllite. Relict clasts and minerals in semischist also include anhedral pleochroic brown hornblende (0–10%) and mafic metavolcanic clasts (0–10%) that contain various combinations of actinolite, chlorite, and epidote (0–5%), homogeneous chlorite clots (0–1%), and (or) microlitic plagioclase lathwork volcanic clasts in an aphanitic matrix (0–2%). Pelitic to semipelitic rip-up clasts occur in most samples (0–5%) and rarely contain fine lawsonite needles[1]. We did not observe any detrital augite in the semischist of Mount Josephine.

Jsh_s **Shuksan Greenschist (Jurassic)**—Mostly epidote ± actinolite-bearing metabasalt, metabasaltic andesite, and rarely andesitic greenschist; mostly greenish gray to gray-green, also medium bluish gray to light greenish gray, weathering to a light olive gray; strongly S1 foliate; dominant metamorphic minerals include polygonal and granoblastic quartz (0–20%, avg. 7%) and albite (10–35%, avg. 24%; includes relict plagioclase laths), with xenoblastic and typically coarse-grained actinolite (0–45%, avg. 19%), epidote (4–40%, avg. 18%) (locally porphyroblastic), Fe-chlorite (0–20%, avg. 4%), Mg-chlorite (0–39%, avg. 15%). Lesser metamorphic minerals include Al-pumpellyite (0–15%, avg. 3%), muscovite (0–33%, avg. 3%), and calcite (0–20%, avg. 3%). Relict igneous minerals include locally sausseritized, albitized, euhedral to subhedral plagioclase laths (0.2–2 mm in diameter) and corroded, anhedral or actinolized hornblende (typically 1–2 mm in diameter; 0–5%, avg. 1%). Accessory minerals include titanite (0–5%, avg. 1%), opaques (0–1%), and iron oxides (0–2%). Locally, the greenschists contain 'epidote-rich knots' or segregations rich in xenoblastic porphyroblasts of epidote that surround other phases such as plagioclase. (See Haugerud and others, 1981, for epidote segregations and knots in the Easton suite.)

A meter-thick pod of S1-foliate(?) quartz (~35%), talc (~60%), and Mg-chlorite (~5%) occurs between greenschist, metachert, and phyllite (Fig. 4, site 72S). The site is similar to a quarry in our Lyman Hill fault zone (Fig. 4, directly east of site 6J) where Gallagher (1986) and Gallagher and others (1988) describe interlayered and S1 foliate ultramafite, metatuffaceous greenschist, and phyllite that were interpreted to be interleaved prior to D1. (We were unable to locate this site in this quarry.) Site 72S may support Gallagher and others (1988) contention that the Easton suite in the area contains primary ultramafic detritus of seafloor origin.

[1] Lawsonite (orthorhombic) was distinguished from pumpellyite (monoclinic) by the straight extinction of lawsonite versus the +22° extinction of pumpellyite on (100) cleavage. Lawsonite occurs as nonpleochroic, euhedral, fine rectangular tabular crystals that have rhombic cross sections with good (010) and (001) cleavage; pumpellyite generally occurs as pleochroic crystals of varied form or habit (generally fibrous) with moderate (001) and (100) cleavage (Kerr, 1977).

MESOZOIC METAMORPHIC ROCKS OF THE HAYSTACK THRUST NAPPE OF WHETTEN AND OTHERS (1980b, 1988) OR THE HELENA–HAYSTACK MÉLANGE OF TABOR (1994)

Geologists attempting tectonic and structural syntheses in the lower Skagit River area of the Northwest Cascades system are faced with a bewildering profusion of nappe and rock assemblage correlations and resulting structural thrust stratigraphy interpretations. Previous studies of the Northwest Cascades system of the lower Skagit River area, some of which covered the study area in a reconnaissance manner, are listed and discussed in Dragovich and others (1998), who noted the contradictory interpretations of many of these studies.

We correlate blocks of greenstone and metasedimentary rock in a serpentinite-matrix mélange overlying the Shuksan metamorphic suite with the Helena–Haystack mélange (HH) of Tabor (1994), which is similar to the Haystack thrust nappe concept of Whetten and others (1988). The HH nappe overlies the Shuksan nappe south of the Skagit River (Whetten and others, 1988; Tabor, 1994; fig. 13 of Dragovich and others, 1998) and consists of a mostly chaotic assemblage of ocean-floor (ophiolitic) or island-arc greenstone and metasedimentary rocks with associated ultramafite. The HH, as defined by Tabor (1994), lies north of the Darrington–Devils Mountain fault and south of the Skagit River (fig. 2 of Dragovich and others, in press b). South of the Skagit River, thrusting of the HH over the Shuksan nappe at Table Mountain and to the east near Deer Peak (figs. 5 and 6 of Dragovich and others, in press b) probably occurred in the mid-Cretaceous. Dragovich and others (1998) extended the HH north of the Skagit River.

Tabor (1994) emphasized that the HH contains exotic elements from the upper and lower plates and forms an imbricate zone between the Shuksan nappe and eastern and western mélange belts (fig. 5 of Dragovich and others, in press b). Tabor states "the HH mélange is analogous to the Haystack thrust plate of Whetten and others (1980b) but differs in extent and mode of formation. It represents the bounding fault between the last Mesozoic terranes (the western and eastern mélange belts) to be accreted to North America in the Pacific Northwest."

Three nearly concordant U-Pb zircon age estimates of plagiogranite from the HH directly south-southeast of the study area indicate an intrusive age of about 160 to 170 Ma for the unit (Whetten and others, 1980b, 1988). These ages are similar to U-Pb ages and radiolarian fossil ages from the Fidalgo ophiolite obtained by Brown and others (1979). Tabor (1994) includes the Fidalgo ophiolite in the broadly defined HH. A sample of chert from the Bow quadrangle (Dragovich and others, 1998) contains coarsely recrystallized radiolarians that could not be identified to genus but indicate a questionable Jurassic age (C. D. Blome, USGS, oral commun., 1998). Dragovich and others (1998) obtained a nearly concordant $^{206}Pb/^{238}U$ zircon age of 163.2 ±0.4 Ma and a $^{207}Pb/^{235}U$ zircon age of 162.5 ±3.5 Ma from an HH metagabbroic klippe on Colony mountain west of the present study area.

In the study area, the HH is divided into metavolcanics (unit Jmv_h), metagabbroic greenstone (unit $Jigb_h$), and ultramafite (unit Ju_h). The dominant lithologies of the HH are metabasite (unit Jmv_h) and ultramafite (unit Ju_h). The heterogeneous metamorphic rocks of Skagit valley (unit $Jhmc_h$) are a continuation of the informally named heterogeneous metamorphic rocks of

Butler Hill to the west (Dragovich and others, 1998); these mélange rocks contain metabasaltic to meta-andesitic greenstone and lesser metagabbro; tectonic blocks of phyllitic to slaty meta-argillite, metasandstone, and rare metachert occur locally (Dragovich and others, 1998). A few contacts appear to be primary. For example, north of Sedro-Woolley (Fig. 4, site 24H), a probable unsheared depositional contact between metasedimentary rocks and metabasites suggests that protoliths of the metasedimentary rock of the mélange were deposited with metavolcanic rock of the mélange in an oceanic environment. Mostly, however, HH intraformational contacts are structural and originate from a combination of mélange (subduction?) and (or) younger thrust mechanisms. The various oceanic units are commonly bounded by ultramafite matrix of probable similar age and probable mantle origin. In the Bow and Alger quadrangles (Fig. 1; Dragovich and others, 1998), greenstone (metabasalt and metagabbro) is associated with ultramafite. Fault contacts containing alpine ultramafic bodies are common and are delineated by small pods to mappable tectonic pods or layers of significant extent (Plate 1).

In the study area, alpine ultramafic bodies (tectonically emplaced ultramafic bodies or slivers common in orogenic zones) delineate the thrust fault between the Easton suite and the HH and are interpreted to be mostly absent in the underlying Easton suite in and directly around the study area. Other contacts between the HH and the Easton suite are probably Tertiary high-angle faults, although some of them may be older, syn-thrusting, high-angle faults discussed by Brown (1987). The spatial association of ultramafite with the HH is also supported by recent USGS magnetic maps (Richard Blakely, USGS, written commun., 1999), which show distinct magnetic highs over the HH klippen. These anomalies are due to the serpentinite matrix of the mélange, which contains significant magnetite (Dragovich and others, 1998; Whetten and others, 1980b). For example, the klippen atop Lyman Hill are distinctly associated with positive 100 to 150 nT circular or ovoid-shaped anomalies. The anomalies outline the map occurrences of HH ultramafite and greenstone and provide evidence that these klippen are associated with significant ultramafite of limited vertical extent (R. Blakely, USGS, written commun., 1999). These anomalies show up against the magnetically quiet Easton suite. The few ultramafic bodies that were observed in the Shuksan nappe do not show up on these detailed magnetic maps, implying small pods and layers of little lateral extent. It is possible that these thin bodies in the Easton suite are remobilized pods or layers displaced into the lower plate by Tertiary faulting.

Ultramafite occurs in four fairly distinct field settings:

(1) As small bodies forming intraformational mélange matrix (for example, in unit $Jhmc_h$ near Sedro-Woolley). Generally metavolcanic block dimensions (tens to hundreds of meters or more) are much greater than the thickness of the interleaved ultramafite matrix; individual mélange blocks are typically hundreds of meters to locally more than a kilometer in map extent (Dragovich and others, 1998).

(2) As mappable or smaller tectonic slices concentrated along the thrust contact between the Easton suite and the overlying HH (Schmidt, 1972; Dragovich and others, 1998; this study) (Plate 1; Plate 4, cross sections I and J; also see plate 1 of Dragovich and others, in press b).

(3) As tectonically remobilized ultramafic lenses along high-angle Tertiary faults throughout the study area. Our interpretation is that Tertiary faulting has displaced the weak serpentinite from the nearby HH (1 and 2, above) into the lower Shuksan nappe. For example, serpentinites along the Lyman Hill fault zone are spatially associated with nearby HH greenstones and are interpreted to be HH lenses imbricated into this fault zone. Other high-angle faults contain serpentinite layers and pods, particularly near the HH.

(4) As talc-tremolite schists or serpentinites rarely associated with Shuksan Greenschist.

Structurally, the HH greenstones are massive or heterogeneously mylonitized to protomylonitized. Grain reduction is prominent in the mylonitic zones and is typically concentrated in thin (few mm thick) zones. These gently dipping microshear zones bound nonmylonitic lenses that preserve static metamorphic mineralogy and relict igneous textures. Metamorphic minerals in the lenticular zones are characteristically fine-grained and statically oriented. Dragovich and others (1998, in press b) assigned the mylonitic fabrics to the thrust emplacement of the HH over the Easton metamorphic suite in the mid-Cretaceous.

$Jhmc_h$ **Heterogeneous metamorphic rocks of Butler Hill of Dragovich and others (1998)(Jurassic)**—Metabasalt and metabasaltic andesite and lesser meta-andesite, lesser phyllitic to slaty graphite-bearing, medium-gray and medium dark-gray meta-argillite, and bluish gray metasandstone; locally contains serpentinite pods and layers (see unit Ju_h) and rare metachert. Dominant metamorphic minerals in meta-argillite include fine-grained matrix quartz (17–25%), albite (3–10%), white mica (0–20%, avg. 13%), and Fe-chlorite (0–20%) and minor, very fine-grained possible Mg-chlorite and epidote (0–3%); accessory minerals include graphite (0–12%), calcite or aragonite (0–3%), with unknown dark matrix material (0–15%), iron oxide (0–2%), and rare probable Fe-pumpellyite and prehnite. Angular to subangular to rarely subrounded relict clasts (0.01–0.3 mm in diameter) constitute as much as 30 percent of the rock and consist mostly of monocrystalline quartz, some polycrystalline quartz, lesser plagioclase, and white mica or chlorite (rip-up?) lenticular clots of probable detrital origin. Dominant metamorphic minerals in metasandstone include quartz (5–6%), albite (~5%), white mica (10–12%), chlorite (4–10%), and minor graphite ± iron oxide. Relict clasts (0.1–0.4 mm in diameter) in arkosic metasandstones or feldspathic graywackes constitute about 60 to 75 percent of the rock; clasts include polycrystalline quartz (~40%), plagioclase (~30%), and monocrystalline quartz (~25%), as well as meta-argillite (typically white-mica-rich) rip-up clasts (≤2 mm in diameter) and minor lithic grains (<1 mm in diameter).

Meta-argillite is semipelitic to locally pelitic and occurs as beds typically a few centimeters to decimeters thick in metasandstone or as massive beds between sandstone outcrops. Meta-argillite is also interlayered with meta-andesite on Dukes Hill. Microscopically, bedding is defined by decreased graphite and matrix content and increased clast size from silt or very fine sand to medium sand. Sedimentary structures include local graded bedding from meta-argillite to metasandstone. Metasandstone contains probable rare ripple cross-lamination. Rip-up clasts of meta-argillite are common in the sandstone, and they are commonly larger clasts than the crystal-lithic sand-sized clasts of the unit.

The unit is characterized by a strong phyllitic to slaty cleavage. Local rootless disharmonic folds and disassociated thin quartz veins (<1 mm wide) cut across the cleavage. The quartz veins appear to be shear folded during cleavage formation. Unlike the Easton suite, metasedimentary rock cleavage and bedding are locally distinctly nonparallel, quartzose metamorphic segregations are lacking, and the metasedimentary rocks are less recrystallized. Also, metamorphic minerals are distinctly finer grained, and relict grain outlines are better preserved.

Jmv_h **Metavolcanics of the Helena–Haystack mélange (Jurassic)**—Mostly augite-bearing greenstone (metabasalt and metabasaltic andesite with lesser meta-andesite) and greenstone pillow breccia; locally heterogeneously protomylonitic to mylonitic; metabasaltic and metabasaltic andesitic greenstones are greenish gray to light greenish gray or gray-green and weather to a light olive gray; meta-andesitic greenstones are light greenish gray to dark green-gray.

The metabasaltic and metabasaltic andesitic greenstones consist of albite (20–43%, avg. 30%; includes relict plagioclase laths), acicular fine-grained actinolite (0–45%, avg. 7%), sugary fine-grained matrix epidote (0–25%, avg. 12%; <0.2 mm in diameter), Fe-chlorite (1–15%, avg. 8%), Mg-chlorite (0–32%, avg. 9%); lesser common metamorphic minerals include quartz (0–8%, avg. 3%), stellate or acicular Al-pumpellyite or Fe-pumpellyite (0–25%, avg. 11%), calcite (0–1%), calcite or aragonite (0–4%), and stilpnomelane (17% in one sample). Relict igneous minerals commonly define a preserved hypidiomorphic granular igneous texture; relict igneous grains include locally sausseritized and albitized, euhedral to subhedral plagioclase laths, locally with an acicular habit (0.2–2 mm in diameter), subhedral to euhedral augite (0–25%, avg. 12%; 0.2–1.5 mm in diameter)[1], and euhedral igneous titanite (sphene)(0–2%; ≤2 mm in diameter). The matrix is commonly cloudy and contains unknown aphanitic semi-opaque minerals that are probably recrystallized glass (0–18%, avg. 6%), as well as miscellaneous relict angular igneous fragments; fragments contain microlites of plagioclase surrounded by fine-grained metamorphic minerals in a dark devitrified volcanic matrix. Rounded to elliptical Fe-pumpellyite-filled vesicles are common. Corroded and replaced hornblende and actinolized hornblende (typically ~1 mm long) occur in one sample. Accessory minerals include white mica (1% in 1 sample), titanite (0–6%), and opaques (0–2%), and probable serpentine (1% in 1 sample).

Dominant metamorphic minerals of the andesitic greenstones include albite (25–44%, includes relict plagioclase laths), quartz (10–20%, includes relict phenocrysts), Fe-chlorite (10–15%); lesser metamorphic minerals include white mica (0–10%), stellate or radiating apple-green pleochroic Fe-pumpellyite (4–8%), possible fine-grained prehnite (0–3%), stilpnomelane (4% in 1 sample). Relict igneous minerals include albitized, euhedral to subhedral to locally acicular plagioclase laths (0.1–0.8 mm in diameter), subhedral to euhedral augite (0–15%; ~0.3 mm in diameter), subhedral to anhedral quartz (~0.8 mm in diameter), and subhedral titanite (sphene)(0–3%) that may be a relict igneous phase. Relict angular igneous fragments in meta-andesite include microlites of plagioclase surrounded by a very fine-grained mat of metamorphic minerals in a dark relict volcanic matrix of recrystallized glass. Some of the relict igneous fragments are replaced by a fine-grained radiating mat of acicular actinolite + pumpellyite ± Fe-chlorite. Accessory minerals include opaques (0–1%) and iron oxide (1% in one sample).

Fine-grained actinolite most commonly occurs interstitially as a nonfoliated or semi-aligned matrix phase. Random to foliation-aligned actinolite needles occur in pressure shadows formed during microboudinage or as replacement products of relict hornblende. (Uralitization and production of relict hornblende from augite in a late magmatic stage seems likely.) Aragonite (x-ray determined), calcite, chlorite, and pumpellyite commonly occur as accessory minerals; quartz most commonly occurs in extensional veins. Less common but notable petrologic relations include pumpellyite replacing augite and normally zoned relict plagioclase laths. (See Dragovich and others, in press b, for further microstructural description.)

Pillow structures are common and locally well preserved. Pillow breccia contains angular to subangular clasts in a matrix of similar composition. Some concentric microtextures are probably primary spherulitic or hyalopilitic pillow or pillow breccia. Relict volcanic fragment textures are extremely varied, but most metavolcanics are aphanitic or microlitic and have felty feldspar textures surrounded by a dark recrystallized glass matrix.

$Jigb_h$ **Augite-bearing metagabbro of the Helena–Haystack mélange on Lyman Hill (Jurassic)**—Medium-grained, massive to mylonitic or protomylonitic metagabbro; greenish gray or dark greenish gray. Metamorphic minerals include albitized plagioclase (45–50%, avg. 48%; includes relict plagioclase laths), acicular actinolite (0–6%, avg. 2%), epidote (0–4%, avg. 2%), Fe-chlorite (8–15%, avg. 12%), Mg-chlorite (0–5%, avg. 2%), and stilpnomelane (0–10%, avg. 3%). Dominant relict igneous minerals include mildly to strongly sausseritized plagioclase laths (1–4 mm in diameter) and augite (15–31%, avg. 25%; 1–2.3 mm in diameter). Hypidiomorphic granular in nonfoliated zones, the overall preserved igneous texture is subophitic with some preserved euhedral phenocrysts. Accessory minerals include opaques (0–1%), titanite (4–6%, avg. 5%), and rare clinozoisite or zoisite.

Plagioclase is mostly albitized. Saussuritization of much of the plagioclase suggests that prior to metamorphism the plagioclase was more calcic (>An_{50}?) and melanocratic (dark green) and thus these rocks are categorized as gabbros. Increased saussuritization in

[1] Augite is characteristic of the HH greenstone. This relict phase is areally extensive and occurs in HH metavolcanic rocks of both the klippen and the isolated hillocks of the Skagit valley. Augite has been positively identified in 54 percent of the HH metabasaltic, metabasaltic andesitic, andesitic, and gabbroic greenstone samples studied in the Bow, Alger, Sedro-Woolley North, and Lyman quadrangles (24 of 45 thin-sections). Noteworthy is the observation that this phase has not been identified in any of the samples that we mapped as Shuksan Greenschist.

the cores of a few samples suggests normal igneous plagioclase zonation for these intrusive rocks. Plagioclase is locally replaced by chlorite. Actinolite replaces plagioclase and augite. Metagabbroic rocks are massive to locally mylonitized along flat to gently north-northeast-dipping, few millimeters-thick mylonite zones. The mylonite zones are heterogeneous and bound lenticular zones preserving statically metamorphosed primary hypidiomorphic granular textures (for example, Fig. 4, site 3A). (See Dragovich and others, in press b, for a description of the deformational episodes in the Helena–Haystack mélange.)

Ju_h **Ultramafite of the Helena–Haystack mélange (Jurassic)**—Serpentinite with lesser talc and tremolite-bearing serpentinites, magnesite-veined mylonitic serpentinites containing thick pods and layers of magnesite, mariposite, and rare allotriomorphic-granular-textured, diopside-bearing clinopyroxenites within serpentinite; serpentinites are dark green-gray to greenish black and weather to pale green or a distinctive dark yellowish orange; magnesite veins and bodies are very pale orange and contain dark yellow-orange tectonic clasts of the same mineral and green serpentinite; peridotites are greenish gray. Serpentinites contain serpentine-group minerals with localized veins of chrysotile asbestos (serpentinite minerals 40–82%) with lesser tremolite (0–10%), chlorite (0–15%), and accessory talc (0–20%), magnesite (0–80%, see below), chromite, magnetite, and rare epidote or retrogressed pyroxene ghosts. Serpentinites grade into magnesite-bearing rocks and tectonized magnesite deposits with increased veining in the 'Hamilton klippe' near Mount Josephine (directly west of the study area) (See Dragovich and others, in press b). Pyroxenite (Fig. 4, site 25Z) contains diopside (~80%) with serpentinite and Mg-chlorite (~15%) and accessory pumpellyite.

ACKNOWLEDGMENTS

This report was produced in cooperation with the U.S. Geological Survey National Cooperative Geologic Mapping Program Agreement Number 98-HQ-AG-2062. Field mapping was performed by all the authors. Map compilation, analyses, illustrations, and other documentation were done by Joe Dragovich. Dave Norman helped with compilation and analysis of the geochemical data. Dave Norman and Tom Lapen helped with compilation of the structural data. We greatly thank Keith Ikerd for excellent cartographic support on the map, figures, correlation diagram, and explanations. We are indebted to D. Dethier (Williams College) for providing enlightening discussions and reviewing the manuscript. Rex Davis and Carly Grisamer were our very capable 1998 field assistants. Jason Cass and Minda Troost were our very capable field assistants in 1999 and helped with some field checking. We thank Rowland Tabor (USGS emeritus), E. H. 'Ned' Brown (Western Washington Univ.), and Ralph Haugerud (USGS) for geological insights and discussion. Tabor provided mostly unpublished geochemical samples and data. Richard Blakely (USGS) kindly provided magnetic maps and helped interpret new detailed USGS magnetic survey maps. We appreciate Bill McClelland's (Univ. of Idaho) attempt to date zirconless metagabbro in the study area. We appreciate the assistance of Phil Ambrosino (Washington State Dept. of Transportation Materials Lab.) with our geotechnical boring compilation. Thanks also to DGER staff members Eric Schuster, Josh Logan, and Ray Lasmanis for reviews of the manuscript; Karen Meyers for text layout and editorial help; Jari Roloff for computer drafting, text editing, and layout; Mary Ann Shawver for prepping topographic maps for field use; Connie Manson and Lee Walkling for assistance with references; and Catherine Kenner, Phillip Dobson, and Jan Allen for clerical support.

REFERENCES CITED

Armstrong, J. E., 1981, Post-Vashon Wisconsin glaciation, Fraser Lowland, British Columbia: Geological Survey of Canada Bulletin 322, 34 p.

Armstrong, J. E.; Crandell, D. R.; Easterbrook, D. J.; Noble, J. B., 1965, Late Pleistocene stratigraphic chronology in southwestern British Columbia and northwestern Washington [abstract]: Geological Society of America Special Paper 82, p. 237.

Armstrong, R. L., 1980, Geochronometry of the Shuksan Metamorphic Suite, North Cascades, Washington [abstract]: Geological Society of America Abstracts with Programs, v. 12, no. 3, p. 94.

Armstrong, R. L.; Misch, Peter, 1987, Rb-Sr and K-Ar dating of mid-Mesozoic blueschist and late Paleozoic albite-epidote-amphibolite and blueschist metamorphism in the North Cascades, Washington and British Columbia, and Sr-isotope fingerprinting of eugeosynclinal rock assemblages. *In* Schuster, J. E., editor, Selected papers on the geology of Washington: Washington State Division of Geology and Earth Resources Bulletin 77, p. 85-105.

Balzarini, M. A., 1981, Paleoecology of Everson-age glacialmarine drifts in northwestern Washington and southwestern British Columbia: University of Washington Master of Science thesis, 109 p.

Balzarini, M. A., 1983, Paleoecology of late Pleistocene glacial-marine sediments in northwestern Washington and southwestern British Columbia. *In* Molnia, B. F., editor, Glacial-marine sedimentation: Plenum Press, p. 571-592.

Bechtel, Inc., 1979, Report of geologic investigations in 1978–1979; Skagit Nuclear Power Project: Puget Sound Power and Light Company, 3 v., 3 pl.

Beget, J. E., 1981, Postglacial eruption history and volcanic hazards at Glacier Peak, Washington: University of Washington Doctor of Philosophy thesis, 192 p.

Beget, J. E., 1982, Postglacial volcanic deposits at Glacier Peak, Washington, and potential hazards from future eruptions: U.S. Geological Survey Open-File Report 82-830, 77 p.

Booth, D. B., 1994, Glaciofluvial infilling and scour of the Puget Lowland, Washington, during ice-sheet glaciation: Geology, v. 22, no. 8, p. 695-698.

Booth, D. B.; Hallet, Bernard, 1993, Channel networks carved by subglacial water—Observations and reconstruction in the eastern Puget Lowland of Washington: Geological Society of America Bulletin, v. 105, no. 5, p. 671-683.

Brandon, M. T.; Cowan, D. S.; Vance, J. A., 1988, The Late Cretaceous San Juan thrust system, San Juan Islands, Washington: Geological Society of America Special Paper 221, 81 p., 1 pl.

Brown, E. H., 1986, Geology of the Shuksan Suite, North Cascades, Washington, U.S.A. *In* Evans, B. W.; Brown, E. H., editors, Blueschists and eclogites: Geological Society of America Memoir 164, p. 143-154.

Brown, E. H., 1987, Structural geology and accretionary history of the Northwest Cascades system, Washington and British Columbia: Geological Society of America Bulletin, v. 99, no. 2, p. 201-214.

Brown, E. H.; Bernardi, M. L.; Christenson, B. W.; Cruver, J. R.; Haugerud, R. A.; Rady, P. M.; Sondergaard, J. N., 1981, Metamorphic facies and tectonics in part of the Cascade Range and Puget Lowland of northwestern Washington: Geological Society of America Bulletin, v. 92, no. 4, Part I, p. 170-178.

Brown, E. H.; Blackwell, D. L.; Christenson, B. W.; Frasse, F. I.; Haugerud, R. A.; Jones, J. T.; Leiggi, P. A.; Morrison, M. L.; Rady, P. M.; and others, 1987, Geologic map of the northwest Cascades, Washington: Geological Society of America Map and Chart Series MC-61, 1 sheet, scale 1:100,000, with 10 p. text.

Brown, E. H.; Bradshaw, J. Y.; Mustoe, G. E., 1979, Plagiogranite and keratophyre in ophiolite on Fidalgo Island, Washington: Geological Society of America Bulletin, v. 90, no. 5, p. I 493-I 507.

Brown, E. H.; Wilson, D. L.; Armstrong, R. L.; Harakal, J. E., 1982, Petrologic, structural, and age relations of serpentinite, amphibolite, and blueschist in the Shuksan suite of the Iron Mountain–Gee Point area, North Cascades, Washington: Geological Society of America Bulletin, v. 93, no. 11, p. 1087-1098.

Carlstad, C. A., 1992, Late Pleistocene deglaciation history at Point Partridge, central Whidbey Island, Washington: Western Washington University Master of Science thesis, 1 v.

Clague, J. J., 1980, Late Quaternary geology and geochronology of British Columbia; Part 1, Radiocarbon dates: Geological Survey of Canada Paper 80-13, 28 p.

Clague, J. J., 1981, Late Quaternary geology and geochronology of British Columbia; Part 2, Summary and discussion of radiocarbon-dated Quaternary history: Geological Survey of Canada Paper 80-13, 28 p.

Clague, J. J.; Mathewes, R. W.; Guilbault, J. P.; Hutchinson, Ian; Ricketts, B. D., 1998, Pre-Younger Dryas resurgence of the southwestern margin of the Cordilleran ice sheet, British Columbia, Canada; Discussion and reply: Boreas, v. 27, no. 3, p. 225-230.

Croll, T. C., 1980, Stratigraphy and depositional history of the Deming Sand in northwestern Washington: University of Washington Master of Science thesis, 57 p.

Dethier, D. P.; Pessl, Fred, Jr.; Keuler, R. F.; Balzarini, M. A.; Pevear, D. R., 1995, Late Wisconsinan glaciomarine deposition and isostatic rebound, northern Puget Lowland, Washington: Geological Society of America Bulletin, v. 107, no. 11, p. 1288-1303.

Dethier, D. P.; Whetten, J. T., 1981, Preliminary geologic map of the Mount Vernon 7½-minute quadrangle, Skagit County, Washington: U.S. Geological Survey Open-File Report 81-105, 9 p., 1 pl., scale 1:24,000.

Dethier, D. P.; White, D. P.; Brookfield, C. M., 1996, Maps of the surficial geology and depth to bedrock of False Bay, Friday Harbor, Richardson, and Shaw Island 7.5-minute quadrangles, San Juan County, Washington: Washington Division of Geology and Earth Resources Open File Report 96-7, 7 p., 2 pl.

Dickinson, W. R., 1970, Interpreting detrital modes of graywacke and arkose: Journal of Sedimentary Petrology, v. 40, n. 2, p. 695-707.

Domack, E. W., 1982, Facies of late Pleistocene glacial marine sediments on Whidbey Island, Washington: Rice University Doctor of Philosophy thesis, 312 p., 11 pl.

Domack, E. W., 1983, Facies of late Pleistocene glacial-marine sediments on Whidbey Island, Washington—An isostatic glacial-marine sequence. *In* Molnia, B. F., editor, Glacial-marine sedimentation: Plenum Press, p. 535-570.

Domack, E. W., 1984, Rhythmically bedded glaciomarine sediments on Whidbey Island, Washington: Journal of Sedimentary Petrology, v. 54, no. 2, p. 589-602.

Dragovich, J. D.; Dunn, Andrew; Parkinson, K. T.; Kahle, S. C.; Pringle, P. T., 1997a, Quaternary stratigraphy and cross sections, Nooksack, Columbia, and Saar Creek valleys, Kendall and Deming 7.5-minute quadrangles, western Whatcom County, Washington: Washington Division of Geology and Earth Resources Open File Report 97-4, 13 p., 8 pl.

Dragovich, J. D.; Grisamer, C. L., 1998, Quaternary stratigraphy, cross sections, and general geohydrologic potential of the Bow and Alger 7.5-minute quadrangles, western Skagit County, Washington: Washington Division of Geology and Earth Resources Open File Report 98-8, 29 p., 6 pl.

Dragovich, J. D.; McKay, D. T., Jr.; Dethier, D. P.; Beget, J. E., in press a, Voluminous laharic inundation of the lower Skagit River valley, Washington—A product of a single large mid-Holocene Glacier Peak eruptive episode? [abstract]: Geological Society of America Abstracts with Programs, Cordilleran Section, v. 32.

Dragovich, J. D.; Norman, D. K.; Grisamer, C. L.; Logan, R. L.; Anderson, Garth, 1998, Geologic map and interpreted geologic history of the Bow and Alger 7.5-minute quadrangles, western Skagit County, Washington: Washington Division of Geology and Earth Resources Open File Report 98-5, 80 p., 3 pl.

Dragovich, J. D.; Norman, D. K.; Haugerud, R. A.; Pringle, P. T., 1997b, Geologic map and interpreted geologic history of the Kendall and Deming 7.5-minute quadrangles, western Whatcom County, Washington: Washington Division of Geology and Earth Resources Open File Report 97-2, 39 p., 3 pl.

Dragovich, J. D.; Norman, D, K.; Lapen, T. J.; Anderson, Garth, in press b, Interpreted geologic history of the Sedro-Woolley North and Lyman 7.5-minute quadrangles, western Skagit County, Washington: Washington Division of Geology and Earth Resources Open File Report.

Dragovich, J. D.; Pringle, P. T.; Dunn, Andrew; Parkinson, K. T.; Kahle, S. C., 1997c, Quaternary geologic mapping and stratigraphy in the Deming and Kendall 7.5-minute quadrangles, Whatcom County, Washington—Implications for valley hydrostratigraphy in the foothills of the North Cascades [abstract]. *In* Washington Department of Ecology; Washington Hydrologic Society, Abstracts from the 2nd symposium on the hydrogeology of Washington State: Washington Department of Ecology, p. 18.

Easterbrook, D. J., 1962, Pleistocene geology of the northern part of the Puget Lowland, Washington: University of Washington Doctor of Philosophy thesis, 160 p.

Easterbrook, D. J., 1963, Late Pleistocene glacial events and relative sea-level changes in the northern Puget Lowland, Washington: Geological Society of America Bulletin, v. 74, no. 12, p. 1465-1483.

Easterbrook, D. J., 1969, Pleistocene chronology of the Puget Lowland and San Juan Islands, Washington: Geological Society of America Bulletin, v. 80, no. 11, p. 2273-2286.

Easterbrook, D. J., 1971, Geology and geomorphology of western Whatcom County: Western Washington State College Department of Geology, 68 p.

Easterbrook, D. J., 1976a, Geologic map of western Whatcom County, Washington: U.S. Geological Survey Miscellaneous Investigations Series Map I-854-B, 1 sheet, scale 1:62,500.

Easterbrook, D. J., 1976b, Quaternary geology of the Pacific Northwest. *In* Mahaney, W. C., editor, Quaternary stratigraphy of North America: Dowden, Hutchinson and Ross, p. 441-462.

Easterbrook, D. J., 1979, The last glaciation of northwest Washington. *In* Armentrout, J. M.; Cole, M. R.; Ter Best, Harry, Jr., editors, Cenozoic paleogeography of the western United States: Society of Economic Paleontologists and Mineralogists Pacific Section, Pacific Coast Paleogeography Symposium 3, p. 177-189.

Easterbrook, D. J., 1992, Advance and retreat of Cordilleran ice sheets in Washington, U.S.A.: Geographie physique et quaternaire, v. 46, no. 1, p. 51-68.

Easterbrook, D. J., 1994, Chronology of pre-late Wisconsin Pleistocene sediments in the Puget Lowland, Washington. *In* Lasmanis, Raymond; Cheney, E. S., convenors, Regional geology of Washington State: Washington Division of Geology and Earth Resources Bulletin 80, p. 191-206.

Easterbrook, D. J.; Crandell, D. R.; Leopold, E. B., 1967, Pre-Olympia Pleistocene stratigraphy and chronology in the central Puget Lowland, Washington: Geological Society of America Bulletin, v. 78, no. 1, p. 13-20.

Evans, J. E.; Ristow, R. J., Jr., 1994, Depositional history of the southeastern outcrop belt of the Chuckanut Formation—Implications for the Darrington–Devil's Mountain and Straight Creek fault zones, Washington (U.S.A.): Canadian Journal of Earth Sciences, v. 31, no. 12, p. 1727-1743.

Folk, R. L., 1980, Petrology of sedimentary rocks: Hemphill Publishing Company, 182 p.

Foxall, William, 1976, A geophysical study of the Skagit Valley: University of Washington Master of Science thesis, 88 p.

Gallagher, M. P., 1986, Structure and petrology of meta-igneous rocks in the western part of the Shuksan Metamorphic Suite, northwestern Washington, U.S.A.: Western Washington University Master of Science thesis, 59 p., 3 pl.

Gallagher, M. P.; Brown, E. H.; Walker, N. W., 1988, a new structural and tectonic interpretation of the western part of the Shuksan blueschist terrane, northwestern Washington: Geological Society of America Bulletin, v. 100, no. 9, p. 1415-1422.

Haugerud, R. A., 1980, The Shuksan Metamorphic Suite and Shuksan thrust, Mt. Watson area, North Cascades, Washington: Western Washington University Master of Science thesis, 125 p., 2 pl.

Haugerud, R. A.; Morrison, M. L.; Brown, E. H., 1981, Structural and metamorphic history of the Shuksan Metamorphic Suite in the Mount Watson and Gee Point areas, North Cascades, Washington: Geological Society of America Bulletin, v. 92, no. 6, Part I, p. 374-383.

Heller, P. L., 1978, Pleistocene geology and related landslides in the lower Skagit and Baker valleys, North Cascades, Washington: Western Washington University Master of Science thesis, 154 p., 5 pl.

Heller, P. L., 1981, Small landslide types and controls in glacial deposits—Lower Skagit River drainage, northern Cascade Range, Washington: Environmental Geology, v. 3, no. 4, p. 221-228.

Heller, P. L.; Dethier, D. P., 1981, Surficial and environmental geology of the lower Baker valley, Skagit County, Washington: Northwest Science, v. 55, no. 2, p. 145-155.

Jenkins, O. P., 1924, Geological investigation of the coal fields of Skagit County, Washington: Washington Division of Geology Bulletin 29, 63 p., 2 pl.

Johnson, S. Y., 1982, Stratigraphy, sedimentology, and tectonic setting of the Eocene Chuckanut Formation, northwest Washington: University of Washington Doctor of Philosophy thesis, 221 p., 4 pl.

Johnson, S. Y., 1984, Stratigraphy, age, and paleogeography of the Eocene Chuckanut Formation, northwest Washington: Canadian Journal of Earth Sciences, v. 21, no. 1, p. 92-106.

Johnson, S. Y.; Whetten, J. T.; Naeser, C. W.; Zimmermann, R. A., 1983, Fission track ages from the Chuckanut Formation, northwest Washington [abstract]: Geological Society of America Abstracts with Programs, v. 15, no. 5, p. 393.

Kerr, P. F., 1977, Optical mineralogy; 4th ed.: McGraw-Hill, 492 p.

Klungland, M. W.; McArthur, Michael, 1989, Soil survey of Skagit County area, Washington: U.S. Soil Conservation Service, 372 p., 67 pl.

Kovanen, D. J., 1996, Extensive late-Pleistocene alpine glaciation in the Nooksack River valley, North Cascades, Washington: Western Washington University Master of Science thesis, 186 p.

Kunzler, L. J., 1991, Skagit River valley—The disaster waiting to happen: [Privately published by the author, Seattle, Wash.], 97 p.

Le Bas, M. J.; Le Maitre, R. W.; Streckeisen, A. L.; Zanettin, Bruno, 1986, A chemical classification of volcanic rocks based on the total alkali-silica diagram: Journal of Petrology, v. 27, no. 3, p. 745-750.

Miller, G. M.; Misch, Peter, 1963, Early Eocene angular unconformity at western front of northern Cascades, Whatcom County, Washington: American Association of Petroleum Geologists Bulletin, v. 47, no. 1, p. 163-174.

Misch, Peter, 1966, Tectonic evolution of the northern Cascades of Washington—a west-cordilleran case history. *In* Canadian Institute of Mining and Metallurgy; and others, A symposium on the tectonic history and mineral deposits of the western Cordillera in British Columbia and neighbouring parts of the United States, Vancouver, 1964: Canadian Institute of Mining and Metallurgy Special Volume 8, p. 101-148, 1 pl.

Mustoe, G. E.; Gannaway, W. L., 1997, Paleogeography and paleontology of the early Tertiary Chuckanut Formation, northwest Washington: Washington Geology, v. 25, no. 3, p. 3-18.

Obradovich, J. D., 1994, An updated time scale for the Cretaceous of North America [abstract]: American Association of Petroleum Geologists and Society of Economic Paleontologists and Mineralogists Annual Meeting Abstracts, p. 227.

Pessl, Fred, Jr.; Dethier, D. P.; Booth, D. B.; Minard, J. P., 1989, Surficial geologic map of the Port Townsend 30- by 60-minute quadrangle, Puget Sound region, Washington: U.S. Geological Survey Miscellaneous Investigations Series Map I-1198-F, 1 sheet, scale 1:100,000, with 13 p. text.

Powell, R. D., 1984, Glaciomarine processes and inductive lithofacies modeling of ice shelf and tidewater glacier sediments based on Quaternary examples: Marine Geology, v. 57, no. 1-4, p. 1-52.

Reiswig, K. N., 1982, Palynological differences between the Chuckanut and Huntingdon Formations, northwestern Washington: Western Washington University Master of Science thesis, 61 p.

Rigg, G. B., 1958, Peat resources of Washington: Washington Division of Mines and Geology Bulletin 44, 272 p.

Robertson, C. A., 1981, Petrology, sedimentology, and structure of the Chuckanut Formation, Coal Mountain, Skagit County, Washington: University of Washington Master of Science thesis, 41 p., 2 pl.

Rubin, Meyer; Alexander, Corrinne, 1958, U.S. Geological Survey radiocarbon dates IV: Science, v. 127, no. 3313, p. 1476-1487.

Salvador, Amos, 1985, Chronostratigraphic and geochronometric scales in COSUNA stratigraphic correlation charts of the United States: American Association of Petroleum Geologists Bulletin, v. 69, no. 2, p. 181-189.

Schmidt, S. L., 1972, Geology of the south part of Chuckanut Mtn., a structural and petrological study: Western Washington State College Master of Science thesis, 51 p., 1 pl.

Siegfried, R. T., 1978, Stratigraphy and chronology of raised marine terraces, Bay View Ridge, Skagit County, Washington: Western Washington University Master of Science thesis, 52 p., 1 pl.

Stoffel, K. L., 1980, Stratigraphy of pre-Vashon Quaternary sediments applied to the evaluation of a proposed major tectonic structure in Island County, Washington: U.S. Geological Survey Open-File Report 81-292; Washington Division of Geology and Earth Resources Open File Report, 161 p.

Streckeisen, A. L., 1973, Plutonic rocks—Classification and nomenclature recommended by the IUGS Subcommission on the Systematics of Igneous Rocks: Geotimes, v. 18, no. 10, p. 26-30.

Tabor, R. W., 1994, Late Mesozoic and possible early Tertiary accretion in western Washington State—The Helena–Haystack mélange and the Darrington–Devils Mountain fault zone: Geological Society of America Bulletin, v. 106, no. 2, p. 217-232, 1 pl.

Tabor, R. W.; Booth, D. B.; Vance, J. A.; Ford, A. B.; Ort, M. H., 1988, Preliminary geologic map of the Sauk River 30 by 60 minute quadrangle, Washington: U.S. Geological Survey Open-File Report 88-692, 50 p., 2 pl.

Tabor, R. W.; Frizzell, V. A., Jr.; Booth, D. B.; Waitt, R. B.; Whetten, J. T.; Zartman, R. E., 1993, Geologic map of the Skykomish River 30- by 60-minute quadrangle, Washington: U.S. Geological Survey Miscellaneous Investigations Series Map I-1963, 1 sheet, scale 1:100,000, with 42 p. text.

Tabor, R. W.; Haugerud, R. A.; Booth, D. B.; Brown, E. H., 1994, Preliminary geologic map of the Mount Baker 30- by 60-minute quadrangle, Washington: U.S. Geological Survey Open-File Report 94-403, 55 p., 2 pl.

Varnes, D. J., 1958, Landslide types and processes. *In* Eckel, E. B., editor, Landslides and engineering practice: Highway Research Board Special Report 29, p. 20-47.

Varnes, D. J., 1978, Slope movement types and processes. *In* Schuster, R. L.; Krizek, R. J., editors, Landslides—Analysis and control: National Research Council Transportation Research Board Special Report 176, p. 11-33.

Whetten, J. T.; Carroll, P. I.; Gower, H. D.; Brown, E. H.; Pessl, Fred, Jr., 1988, Bedrock geologic map of the Port Townsend 30- by 60-minute quadrangle, Puget Sound region, Washington: U.S. Geological Survey Miscellaneous Investigations Series Map I-1198-G, 1 sheet, scale 1:100,000.

Whetten, J. T.; Dethier, D. P.; Carroll, P. R., 1979, Preliminary geologic map of the Clear Lake NE quadrangle, Skagit County, Washington: U.S. Geological Survey Open-File Report 79-1468, 10 p., 2 pl., scale 1:24,000.

Whetten, J. T.; Dethier, D. P.; Carroll, P. R., 1980a, Preliminary geologic map of the Clear Lake NW quadrangle, Skagit County, Washington: U.S. Geological Survey Open-File Report 80-247, 13 p., 2 pl., scale 1:24,000.

Whetten, J. T.; Zartman, R. E.; Blakely, R. J.; Jones, D. L., 1980b, Allochthonous Jurassic ophiolite in northwest Washington: Geological Society of America Bulletin, v. 91, no. 6, p. I 359-I 368.

Zanettin, Bruno, 1984, Proposed new chemical classification of volcanic rocks: Episodes, v. 7, no. 4, p. 19-20. ■

Appendix 1. Radiocarbon ages, this study

^{14}C analyses performed by Beta Analytic, Inc. (Miami, Fla.). Sample locations shown on Figure 4. Dates are reported as radiocarbon years before present (yr B.P.) (present = A.D. 1950). We report the uncalibrated ages in the text. The quoted results are calibrated to calendar years in the graphs below. By international convention, the modern reference standard was 95 percent of the ^{14}C content of the National Bureau of Standards' oxalic acid and calculated using the Libby ^{14}C half-life (5,568 years). Quoted errors represent 1 standard deviation (68 percent probability) and are based on combined measurements of the sample, background, and modern reference standards. Measured $^{13}C/^{12}C$ ratios were calculated relative to the PDB-1 international standard, and the radiocarbon years before present ages were normalized to -25 per mil.

Sample # 98-42P3: Unit Qoa (Qvl?)

Detrital wood (probable cedar; 18 gm) in clayey silt with gravel (dacite-clast rich with minor phyllite). Found in a 2-m- (7-ft)-deep drainage ditch along the eastern property boundary of the Riggin Room Restaurant in the City of Lyman. Sample depth is 0.9 m (3 ft). Young age indicates that the unit is fill material and that the diamicton is of questionable laharic origin.

Measured ^{14}C age (yr B.P.)	$^{13}C/^{12}C$ ratio	Conventional ^{14}C age (yr B.P.)
100 ±60	-21.9‰	150±60

Beta-125992
Analysis: radiometric standard
Material (pretreatment): wood (acid/alkali/acid)
Location: Fig. 4, site 42P3 (near Lyman)

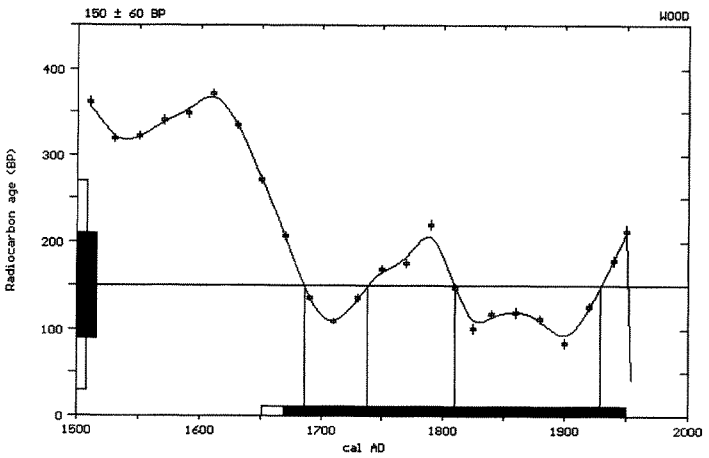

Sample # 98-90A: Unit Qaf

Peat (64 gm) sampled from a paleosol (1–2 cm) overlying clayey diamicton of probable debris-flow origin (south-derived origin probable). Paleosol composed of sticks, charred wood, and disseminated organics. Debris flow is underlain by sand that is exposed at creek level. Paleosol is overlain by a thin- to medium-bedded sequence of sands, silts, and paleosols. Sample is located about 5 m (20 ft) below the terrace surface. Alluvial fan is dissected by the unnamed creek directly east and parallel to Sorenson Creek. ^{14}C age may provide a limiting age for the diamicton lahar and (or) hyperconcentrated volcanogenic flood deposits inferred to reside under this alluvial fan complex. ^{14}C age is younger than the unpublished ^{14}C age of 4,780 yr B.P. (D. Dethier, Williams College, written commun., 1999) obtained from wood in pumiceous lapilli-rich hyperconcentrated flood deposits (unit Qoa) northeast of 90A (Fig. 4, USGS ^{14}C). Stratigraphy and age data suggest that the uppermost portion of the terrace directly south of the Lyman quadrangle contains post-laharic fluvial sediments derived from fluvial-alluvial fan deposits from the Sorenson Creek drainages. It is less likely that the Sorenson Creek samples are Skagit valley flood vertical-accretion deposits. Age is interpreted to date alluvial fan sedimentation onto the Qoa surface after laharic deposition at about 5 ka.

Measured ^{14}C age (yr B.P.)	$^{13}C/^{12}C$ ratio	Conventional ^{14}C age (yr B.P.)
3,850±70	-26.9‰	3,820±70

Beta-125993
Analysis: radiometric standard
Material (pretreatment): peat (acid/alkali/acid)
Location: Fig. 4, site 90A (cut bank of the creek directly east of, and parallel to, Sorenson Creek and directly south of the Lyman 7.5-minute quadrangle)

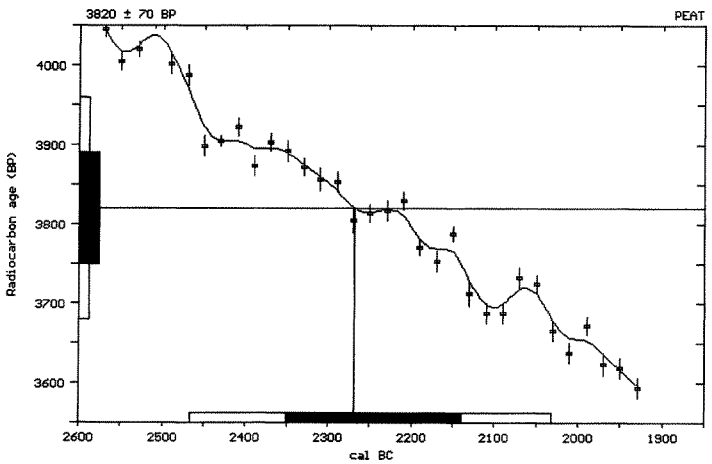

Sample # 98-90D: Unit Qaf

Peat (633 gm) sampled from a peat (~1 m [3 ft] thick) interbedded with silts, sands, and minor gravels with thin paleosols. Exposed unit Qaf sequence is moderately to thinly bedded. Peat composed of sticks, twigs, and disseminated organics. Peat is about 5 m (20 ft) below the top of the alluvial-fan complex and about 3 m (10 ft) above the creek (creek directly east of, and parallel to, Sorenson Creek) that dissects the complex. ^{14}C age may provide a limiting age for the diamicton lahar and (or) hyperconcentrated volcanogenic flood deposits inferred to reside under the alluvial fan complex. ^{14}C age is younger than the unpublished ^{14}C age of 4,780 yr B.P. (D. Dethier, Williams College, written commun., 1999) obtained from pumice lapilli northeast of 90A (Fig. 4, USGS ^{14}C). Stratigraphy and age data suggest that the uppermost portion of the terrace directly south of the Lyman quadrangle contains post-laharic fluvial sediments derived from fluvial-alluvial fan deposits from creek directly east of, and parallel to, Sorenson Creek. It is less likely that these sediments are Skagit valley flood vertical accretion deposits. Age is interpreted to date post-laharic deposition and formation of the Qoa surface after laharic deposition at about 5 ka.

Measured ^{14}C age (yr B.P.)	$^{13}C/^{12}C$ ratio	Conventional ^{14}C age (yr B.P.)
4,150±70	-26.8‰	4,120±70

Beta-125994
Analysis: radiometric standard
Material (pretreatment): peat (acid/alkali/acid)
Location: Fig. 4, site 90D (southernmost Lyman quadrangle)

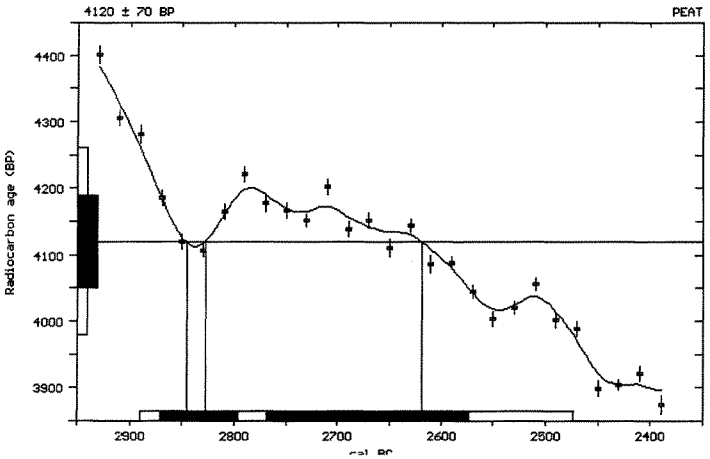

Sample # 98-19A1: Unit Qls

Wood (~10 gm) derived from the outer portion of a log within a silty sandy gravel landslide deposit along the South Fork Nooksack River. Landslide deposit exposed in a the cutbank of the south fork about 12 m (40 ft) above the flood plain. Landslide deposit overlies probable recessional lake deposits of the Everson Interstade (unit Qgl_e). Age provides a limiting age of the landslide deposit.

Measured ^{14}C age (yr B.P.)	$^{13}C/^{12}C$ ratio	Conventional ^{14}C age (yr B.P.)
3,260±70	-26.7‰	3,230±60

Beta-123836
Analysis: radiometric standard
Material (pretreatment): wood (acid/alkali/acid)
Location: Fig 4, site 19A1 (northern Lyman quadrangle and the South Fork Nooksack River)

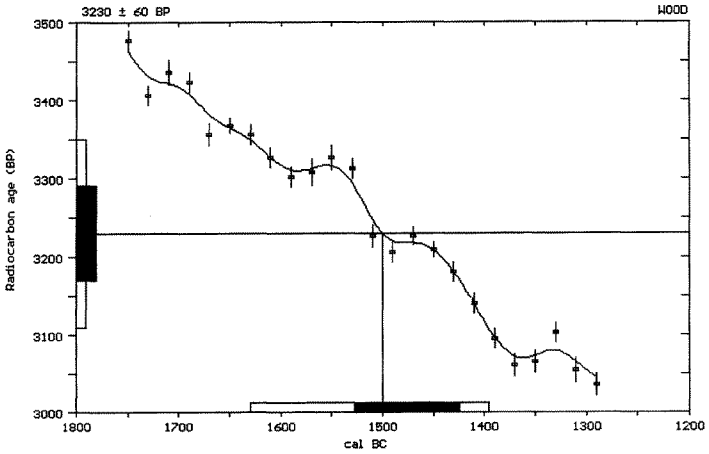

Appendix 2. Major and minor element geochemical analyses, this study

Major, minor, and trace element geochemical analyses of rock units and unit Qoa (lahar run-out) dacite clasts in the Sedro-Woolley North and Lyman quadrangles (this study). Appendix is divided into two sections: (**A**) geochemical sample petrographic and other information, and (**B**) unnormalized and normalized geochemical data. Sample locations shown in Figure 4. See appendix 4 in Dragovich and others, in press b, for rock unit geochemical discrimination diagrams and spidergrams. All analyses are Rigaku x-ray fluorescence and ICP analyses performed at the Geology Department, Washington State University (WSU), Pullman, WA 99164, under the direction of Diane Johnson. Major elements are normalized on a volatile-free basis, with total Fe expressed as FeO. An R after a sample number indicates a rerun or duplicate bead made from the same rock powder; A, average of two runs; †, values >120% of WSU highest standard. A description of the method and estimates of the precision and accuracy are given in Hooper and others (1993). LOI, loss on ignition (roughly reflects the water content and alteration); *, weight percent.

A. GEOCHEMICAL SAMPLE PETROGRAPHIC AND OTHER INFORMATION

Sample no.	SiO_2*	TiO_2*	Geologic unit (rock type)	Location (see Fig. 4)	Phenocrysts or relict clasts	Notes
HELENA–HAYSTACK MÉLANGE METAVOLCANICS AND EASTON METAMORPHIC SUITE METAVOLCANICS AND SEMISCHIST						
2H2	67.21	0.66	Jph_j (semischistose metasandstone)	SWN quad; SW Lyman Mtn.	hornblende, plagioclase, quartz, possible sed. lithic clasts	clasts to 2 cm; granoblastic polygonal matrix texture with albite, chlorite, calcite, epidote, and abundant quartz and minor actinolite; strong S1-S2 metamorphic fabric; metamorphic minerals relatively coarse grained (up to 1mm)
2K	52.12	1.38	Jmv_h (metabasaltic greenstone)	SWN quad; hospital pit	plagioclase	thin heterogeneous mylonitic zones; metamorphic minerals include albite, acicular actinolite, chlorite, and epidote(?); fine-grained metamorphic minerals; mostly static metamorphic recrystallization
2O	46.46	0.38	Jsh_s (metabasaltic greenschist)	SWN quad; SW Lyman Mtn.	plagioclase	metamorphic minerals include albite, chlorite, coarse epidote, and actinolite; penetrative synmetamorphic recrystallization
2P	53.61	0.30	Jsh_s (metabasaltic andesitic greenschist)	SWN quad; SW Lyman Mtn.	sausseritized plagioclase, hornblende	metamorphic minerals include albite, coarse-grained epidote, actinolite, pumpellyite, and minor chlorite; syntectonic recrystallization pervasive
3A	50.11	1.70	$Jigb_h$ (metagabbroic greenstone)	SWN quad; klippe; top of Lyman Mtn.	plagioclase, augite	intrusive texture overprinted by flat inhomogeneous mylonitic fabric; metamorphic minerals include albite, chlorite, actinolite, stilpnomelane, and sphene
4O	47.86	0.68	Jsh_s (metabasaltic greenschist)	SWN quad; SW Lyman Mtn.	probable plagioclase and hornblende relicts	strong S1 fabric with metamorphic segregations (epidote- and albite-rich segregations); granoblastic; albite, chlorite, epidote, and sphene and probable pumpellyite
6J	51.15	2.04	Jmv_h (metabasaltic greenstone)	SWN quad; hospital pit	see nearby sample 2K	see nearby sample 2K
12B	54.72	1.89	Jmv_h (metabasaltic andesitic greenstone)	Lyman quad; klippe	see nearby sample 12C	see nearby sample 12C
12C	51.00	1.63	Jmv_h ($Jigb_h$?) (metabasaltic greenstone)	Lyman quad; klippe	plagioclase, augite, rare hornblende	poorly recrystallized and massive with primary hypidiomorphic granular texture; metamorphic minerals include albite, chlorite, epidote, and sphene; semirandom primary plagioclase relicts; inhomogeneous flat-lying S3 cleavage
15Q	61.59	0.52	$Jhmc_h$ (andesitic greenstone) (metatuff?)	SWN quad; north of Sedro-Woolley	abundant plagioclase, minor quartz	foliation is subparallel to metamorphic fabric in adjacent slate (unit $Jhmc_h$); metamorphic minerals include albite, chlorite, and epidote; high LOI and secondary calcite suggest mineralization and alteration of sample
15R	49.71	1.64	Jmv_h (metabasaltic greenstone)	SWN quad; northernmost Sedro-Woolley	no thin section	massive outcrop contains distinct pillows
16C	68.60	0.74	Jph_j (semischistose metasandstone interlayered with metasiltstone)	Lyman quad; Miner Mtn.	plagioclase and quartz relict detrital clasts	granoblastic polygonal matrix texture; metamorphic minerals include albite, chlorite, and abundant quartz; locally mylonitized along S2 or S3 with disassociated S0
24G	66.70	0.49	Jmv_h (tuffaceous andesitic greenstone)	SWN quad; northernmost Sedro-Woolley	abundant plagioclase, minor augite	metamorphic minerals include chlorite, albite, static acicular actinolite, and possible fine-grained epidote or sphene; possible relict pillows; interlayered with metasiltstone; probable metachert deposited on relict pillows; compositionally similar to sample 15Q (above)

Sample no.	SiO_2*	TiO_2*	Geologic unit (rock type)	Location (see Fig. 4)	Phenocrysts or relict clasts	Notes
24M	49.26	2.35	Jmv_h (metabasaltic greenstone)	SWN quad; northernmost Sedro-Woolley	no thin section; nearby sample 24T contains augite, plagioclase, sphene, and relict vesicles	probable pillows; metamorphic minerals of nearby sample 24T include Fe-chlorite, pumpellyite, stilpnomelane, epidote, and albite
24S	51.47	2.58	Jmv_h (metabasaltic greenstone)	SWN quad; northernmost Sedro-Woolley	no thin section	definite pillows
25B	33.35	1.81	Ju_h (serpentinite)	Lyman quad; klippe; top of Lyman Mtn.	NA	serpentine with lesser tremolite and chlorite; minor magnesite and opaque minerals
25Z	51.50	0.25	Ju_h (diopside-bearing pyroxenite)	SWN quad; klippe; northern Lyman Mtn.	diopside	relict diopside surrounded by lesser serpentine and chlorite; altered or metasomatized zones contain tremolite, amphibole (hornblende?), and chlorite with accessory carbonate (magnesite?) and sphene
25Z2	57.42	0.87	Jmv_h (metabasaltic greenstone)	SWN quad; klippe; northern Lyman Mtn.	no thin section	
31AA1	29.85	2.60	Ju_h (serpentinite)	SWN quad; northern Lyman Mtn.		serpentine with talc, tremolite, and magnesite; contains very gently dipping mylonitic S3 foliation
31AP1	44.79	0.65	Jsh_s (metabasaltic greenschist)	SWN quad; NE Lyman Mtn.	plagioclase	greenschist interlayered with phyllite; very strong S1/L1 fabric; metamorphic minerals include albite, quartz, white mica, chlorite, epidote, and sphene; strongly recrystallized
32A	58.43	0.79	Jmv_h (meta-andesitic greenstone) (locally crystal-vitric tuff?)	Acme quad (Fig. 6); northern Lyman Mtn.	augite, plagioclase, microlitic volcanic clasts, possible relict quartz	massive with static metamorphic recrystallization (fine-grained metamorphic minerals); poorly recrystallized and contains abundant preserved delicate primary volcanic features including semi-opaque relict volcanic clasts (semi-recrystallized volcanic glass fragments?); metamorphic minerals include albite, Fe-chlorite, acicular actinolite, pumpellyite, and possible prehnite with fine grains of epidote; pillows preserved
34L	53.22	1.29	Jmv_h? (metabasaltic andesitic greenstone)	SWN quad; probable erratic; bank of Samish River	plagioclase, augite	metamorphic minerals include Fe-chlorite, epidote, and calcite (aragonite?); nearby sample contains x-ray-determined aragonite
41R	48.36	2.27	Jsh_s(?) (metabasaltic greenstone)	Acme quad; klippe; top of Eddys Mtn. (Fig. 6)	plagioclase	moderately recrystallized with fine-grained metamorphic minerals in a cloudy or semi-opaque matrix; metamorphic minerals include albite, chlorite, pumpellyite, and sphene; systematic (D3?) synmetamorphic veins contain syntaxial actinolite and introduced quartz
42Q	58.44	0.76	Jmv_h (meta-andesitic greenstone; tuffaceous?)	SWN quad; northernmost Sedro-Woolley (Dukes Hill)	plagioclase, quartz (?)	massive or very weak mineral alignment; static recrystallization; metamorphic minerals include albite, chlorite, pumpellyite, white mica, stilpnomelane, and possible prehnite
46Q	51.62	1.67	Jsh_s (metabasaltic greenschist)	Lyman quad; Baucus Hill	no thin section but near greenschist sample 61J	strongly developed, granoblastic, penetrative S1 fabric
47I	50.28	2.38	Jmv_h (metabasaltic greenstone breccia)	Hamilton quad; greenstone klippe (plate 1 of Dragovich and others, in press b)	augite; plagioclase (also occurs as delicate microporphyritic microlites); vesicular	fine-grained, cloudy or semi-opaque, poorly recrystallized matrix with primary igneous features apparent; metamorphic minerals include albite, with mostly static chlorite, pumpellyite, and fine-grained epidote; inhomogeneous thin mylonitic zones defining spaced flat S3 foliation surfaces; syn-D3 veining
47J	52.45	1.76	Jmv_h (metabasaltic andesitic greenstone)	Hamilton quad; greenstone klippe (plate 1 of Dragovich and others, in press b); quarry	no thin section but near sample 47I	mostly massive with an inhomogeneous, shallowly northeast-dipping fracture or fracture cleavage
50C	53.87	1.41	Jsh_s (metabasaltic andesitic greenschist)	SWN quad; SW Lyman Mtn.	plagioclase (near sample 50D)	strongly recrystallized; strong penetrative S1 fabric; protomylonitization of fabric may be due to Tertiary(?) faulting and emplacement of adjacent serpentinite-talc body (few meters north); metamorphic minerals include albite, chlorite, pumpellyite, zoisite, and sphene; geochemistry is suspect (high LOI and post-metamorphic[?] chloritization)
50D	56.73	0.89	Jsh_s (metabasaltic andesitic greenschist)	SWN quad; SW Lyman Mtn.	plagioclase, mostly actinolized hornblende (near sample 50C)	strongly recrystallized; strong penetrative S1/L1 fabric; granoblastic with incipient quartzo-feldspathic segregations; relatively coarse-grained metamorphic minerals (for example, actinolite up to 2 mm long); metamorphic minerals include albite, chlorite, actinolite, epidote, sphene; quartz (15%) abundance is consistent with intermediate composition

Sample no.	SiO_2*	TiO_2*	Geologic unit (rock type)	Location (see Fig. 4)	Phenocrysts or relict clasts	Notes
50I	59.16	0.58	Jsh_s (metatuffaceous(?) andesitic greenschist)	SWN quad; SW Lyman Mtn.	plagioclase	S1 fabric concordant with adjacent phyllite; strongly recrystallized; strong penetrative S1-L1 fabric (some protomylonitization along S1); granoblastic with quartzo-feldspathic segregations or veining parallel to S1; relatively coarse-grained metamorphic minerals; metamorphic minerals include albite, chlorite, epidote, and sphene; geochemistry is suspect (high LOI and post-metamorphic[?] or secondary calcite)
56W	69.43	0.87	Jph_j (semischistose metasandstone)	Lyman quad; Miners Mtn.	no thin section	outcrop displays strong planar S1 fabric
59M	73.17	0.62	Jph_j (semischistose metasandstone interlayered with metasiltstone; graded and planar bedded parallel to S1; turbidites?)	Lyman quad; Miner Mtn.	plagioclase, monocrystalline and polycrystalline relict quartz clasts	granoblastic polygonal matrix texture with albite, white mica, chlorite, epidote, and quartz; rare lenticular chloritic zones may be relict lithic clasts; probable semimature to mature meta-arenite suggested by high relict quartz and plagioclase content
68H	46.24	1.38	Jsh_s (metabasaltic greenschist)	SWN quad; SW Lyman Mtn.	plagioclase, actinolized hornblende	granoblastic polygonal texture with relatively coarse-grained metamorphic minerals; metamorphic minerals include albite, chlorite, epidote, actinolite, sphene, and minor quartz; epidote porphyroblasts (up to 1 mm in diameter); moderately developed S1 foliation
68I	48.10	0.36	Jsh_s (metabasaltic greenschist)	SWN quad; SW Lyman Mtn.	no thin section; but sample near 68H	
69S	50.36	3.21	Jsh_s (protomylonitized metabasaltic greenschist)	SWN quad; S. Lyman Mtn. near thrust-fault contact with Helena–Haystack mélange	plagioclase	greenschist interlayered with Darrington Phyllite; contains moderately strong, flat, protomylonitic S3 fabric; metamorphic minerals include albite, Fe-chlorite, Mg-chlorite, epidote, actinolite, calcite, and sphene; S3 fabric is retrogressive; pumpellyite occurs in syn-D3 veins
U-PB2	51.48	1.75	$Jigb_h$ (metagabbroic greenstone)	SWN quad; klippe; top of Lyman Mtn.	plagioclase; augite (1–2 mm)	intrusive texture locally overprinted by very gently dipping inhomogeneous mylonitic fabric; albite, chlorite, actinolite, sphene; sample zirconless
DACITE CLASTS IN OLDER ALLUVIUM						
42P1	64.53	0.59	Qoa (dacite clasts in hyperconcentrated flood deposit)	Lyman quad; City of Lyman	hypersthene; hornblende; minor quartz	vesicular dacites of similar composition at three Qoa sites strongly suggest a Glacier Peak eruptive precursor to lahar deposits around Lyman
42P2	63.95	0.59	Qoa (dacite clasts in hyperconcentrated flood deposit)	Lyman quad; City of Lyman	hypersthene; hornblende; minor quartz	vesicular dacites of similar composition at three Qoa sites strongly suggest a Glacier Peak eruptive precursor to lahar deposits around Lyman
42P3	63.81	0.59	Qoa (dacite clasts in hyperconcentrated flood deposit)	Lyman quad; City of Lyman	hypersthene; hornblende; minor quartz	vesicular dacites of similar composition at three Qoa sites strongly suggest a Glacier Peak eruptive precursor to lahar deposits around Lyman
75S	64.35	0.63	Qoa (dacite clasts in hyperconcentrated flood deposit)	Lyman quad; north of Minkler Lake (Highway 20)	hypersthene; hornblende; minor quartz	vesicular dacites of similar composition at three Qoa sites strongly suggest a Glacier Peak eruptive precursor to lahar deposits around Lyman
79P1	66.16	0.57	Qoa (dacite clasts in hyperconcentrated flood deposit)	Lyman quad; north of Minkler Lake (Highway 20)	hypersthene; hornblende; minor quartz	vesicular dacites of similar composition at three Qoa sites strongly suggest a Glacier Peak eruptive precursor to lahar deposits around Lyman
79P2	65.69	0.57	Qoa (dacite clasts in hyperconcentrated flood deposit)	Lyman quad; north of Minkler Lake (Highway 20)	hypersthene; hornblende; minor quartz	vesicular dacites of similar composition at three Qoa sites strongly suggest a Glacier Peak eruptive precursor to lahar deposits around Lyman
79P2-2	65.16	0.58	Qoa (dacite clasts in hyperconcentrated flood deposit)	Lyman quad; north of Minkler Lake (Highway 20)	hypersthene; hornblende; minor quartz	vesicular dacites of similar composition at three Qoa sites strongly suggest a Glacier Peak eruptive precursor to lahar deposits around Lyman
79P2-3	66.46	0.54	Qoa (dacite clasts in hyperconcentrated flood deposit)	Lyman quad; north of Minkler Lake (Highway 20)	hypersthene; hornblende; minor quartz	vesicular dacites of similar composition at three Qoa sites strongly suggest a Glacier Peak eruptive precursor to lahar deposits around Lyman

B. GEOCHEMICAL DATA

MAJOR ELEMENTS UNNORMALIZED RESULTS (WEIGHT PERCENT)

Sample no.	Geologic unit (rock type)	LOI (%)	SiO_2	Al_2O_3	TiO_2	FeO	MnO	CaO	MgO	K_2O	Na_2O	P_2O_5	Total
HELENA–HAYSTACK MÉLANGE METAVOLCANIC ROCKS AND EASTON METAMORPHIC SUITE METAVOLCANIC ROCKS AND SEMISCHISTS													
2H2	Jph_j (semischistose metasandstone)	3.79	66.08	11.67	0.645	5.96	0.119	5.24	5.06	1.21	2.20	0.130	98.31
2K	Jmv_h (metabasaltic greenstone)	2.94	51.48	16.93	1.360	7.74	0.132	9.47	6.39	0.20	4.89	0.177	98.76
2K rerun	Jmv_h (metabasaltic greenstone)	2.94	51.54	16.97	1.364	7.57	0.132	9.48	6.38	0.20	4.88	0.176	98.69
2K avg.	Jmv_h (metabasaltic greenstone)	2.94	51.51	16.95	1.36	7.65	0.132	9.48	6.38	0.20	4.88	0.18	98.73
2O	Jsh_s (metabasaltic greenschist)	2.24	45.51	15.92	0.377	11.27	0.117	14.46	8.68	0.02	1.58	0.014	97.95
2P	Jsh_s (metabasaltic andesitic greenschist)	3.27	52.90	18.62	0.300	7.81	0.149	4.48	7.76	1.39	5.24	0.022	98.67
3A	$Jigb_h$ (metagabbroic greenstone)	2.65	49.42	14.89	1.674	10.18	0.190	9.45	8.11	1.36	3.19	0.159	98.62
4O	Jsh_s (metabasaltic greenschist)	2.48	46.60	16.03	0.661	12.31	0.206	10.96	7.98	0.35	2.24	0.018	97.36
6J	Jmv_h (metabasaltic greenstone)	3.20	50.56	16.14	2.017	8.77	0.149	7.96	7.64	1.41	3.91	0.281	98.84
12B	Jmv_h (metabasaltic andesitic greenstone)	2.31	54.18	14.96	1.871	8.44	0.248	6.53	6.23	0.15	6.20	0.198	99.01
12C	Jmv_h ($Jigb_h$?) (metabasaltic greenstone)	2.54	50.02	18.75	1.596	11.27	0.206	6.19	3.90	0.02	5.90	0.221	98.07
15Q	$Jhmc_h$ (andesitic greenstone; metatuff?)	4.77	61.09	16.13	0.516	7.51	0.263	3.34	4.03	0.02	6.20	0.092	99.19
15R	Jmv_h (metabasaltic greenstone)	3.03	48.30	13.61	1.594	10.35	0.217	12.54	6.95	0.03	3.42	0.143	97.16
16C	Jph_j (semischistose metasandstone)	2.91	67.91	14.20	0.732	7.64	0.100	0.67	3.00	0.91	3.66	0.160	98.99
24G	Jmv_h (tuffaceous andesitic greenstone)	3.20	65.82	14.71	0.488	3.81	0.194	11.12	1.60	0.41	0.39	0.144	98.69
24M	Jmv_h (metabasaltic greenstone)	2.56	48.45	14.04	2.311	14.64	0.252	8.79	5.43	0.03	4.19	0.222	98.36
24S	Jmv_h (metabasaltic greenstone)	2.01	50.58	12.76	2.531	12.07	0.251	8.53	6.54	0.92	3.83	0.254	98.27
25B	Ju_h (serpentinite)	10.35	32.70	19.11	1.778	15.33	0.305	1.56	27.10	0.00	0.00	0.158	98.04
25Z	Ju_h (diopside-bearing pyroxenite)	3.66	51.50	4.86	0.249	6.52	0.158	15.33	21.12	0.00	0.24	0.023	100.00
25Z2	Jmv_h (metabasaltic greenstone)	2.17	57.50	18.99	0.869	7.67	0.076	2.73	3.41	0.02	8.62	0.260	100.14
31AA1	Ju_h (serpentinite)	12.68	29.32	18.82	2.557	17.90	0.495	5.80	22.94	0.00	0.13	0.244	98.21
31AA1 rerun	Ju_h (serpentinite)	12.68	29.67	18.07	2.505	17.22	0.486	5.71	21.90	0.00	0.37	0.233	96.16
31AA1 avg.	Ju_h (serpentinite)	12.68	29.50	18.44	2.53	17.56	0.49	5.76	22.42	0.00	0.25	0.24	97.18
31AP1	Jsh_s (metabasaltic greenschist)	6.16	44.70	25.26	0.644	5.92	0.144	12.08	7.11	1.55	2.32	0.061	99.79
32A	Jmv_h (meta-andesitic greenstone)	3.29	58.24	14.38	0.785	9.78	0.212	8.18	3.28	0.25	4.47	0.105	99.68
34L	Jmv_h? (metabasaltic andesitic greenstone)	2.27	52.81	15.95	1.284	10.06	0.183	6.62	5.94	0.03	6.23	0.134	99.24
41R	Jsh_s (metabasaltic greenschist)	6.25	47.60	14.38	2.236	9.37	0.163	13.40	5.81	0.21	4.96	0.288	98.42
42Q	Jmv_h (meta-andesitic greenstone) (metatuff?)	2.81	58.06	16.20	0.755	9.64	0.187	3.99	4.51	0.34	5.55	0.116	99.34
46Q	Jsh_s (metabasaltic greenschist)	2.38	51.02	14.98	1.651	10.27	0.185	8.85	7.38	0.02	4.34	0.147	98.85

Sample no.	Geologic unit (rock type)	LOI (%)	SiO_2	Al_2O_3	TiO_2	FeO	MnO	CaO	MgO	K_2O	Na_2O	P_2O_5	Total
47I	Jmv_h (metabasaltic greenstone breccia)	3.78	49.80	14.95	2.361	12.18	0.215	7.65	7.01	0.10	4.55	0.236	99.06
47J	Jmv_h (metabasaltic andesitic greenstone)	2.35	52.03	14.23	1.742	10.19	0.192	8.17	7.33	0.09	5.05	0.179	99.20
50C	Jsh_s (metabasaltic andesitic greenschist)	6.05	53.51	16.27	1.401	11.21	0.281	5.20	10.20	0.00	1.14	0.110	99.32
50D	Jsh_s (metabasaltic andesitic greenschist)	2.22	56.89	17.16	0.891	7.36	0.129	5.36	5.04	0.03	7.23	0.192	100.28
50I	Jsh_s (andesitic greenschist; metatuff?)	3.78	58.74	17.26	0.579	8.72	0.181	3.18	5.26	0.02	5.26	0.091	99.30
56W	Jph_j (semischistose metasandstone)	2.66	68.70	14.16	0.856	6.38	0.103	0.25	3.08	0.72	4.52	0.175	98.95
59M	Jph_j (semischistose metasandstone)	2.67	72.79	12.47	0.612	5.72	0.106	0.47	2.79	0.99	3.43	0.098	99.48
68H	Jsh_s (metabasaltic greenschist)	1.45	45.33	14.69	1.355	11.40	0.199	16.34	7.47	0.02	1.13	0.106	98.04
68I	Jsh_s (metabasaltic greenschist)	1.45	47.45	15.07	0.356	10.28	0.112	15.30	8.47	0.01	1.60	0.013	98.66
69S	Jsh_s (protomylonitized metabasaltic greenschist)	2.88	49.63	14.38	3.162	13.54	0.240	5.94	6.56	0.02	4.72	0.361	98.55
U-Pb2	$Jigb_h$ (metagabbroic greenstone)	2.31	50.89	15.12	1.725	8.82	0.173	11.54	5.90	0.04	4.53	0.113	98.85
DACITE CLASTS IN OLDER ALLUVIUM													
42P1	Qoa (dacite clasts in hyperconcentrated flood deposit)	0.62	64.40	16.62	0.585	4.31	0.083	4.91	2.35	1.96	4.43	0.158	99.81
42P2	Qoa (dacite clasts in hyperconcentrated flood deposit)	0.90	64.02	16.77	0.590	4.39	0.087	5.09	2.54	1.91	4.55	0.157	100.11
42P3	Qoa (dacite clasts in hyperconcentrated flood deposit)	0.72	63.78	17.00	0.589	4.28	0.081	5.24	2.49	1.87	4.46	0.153	99.95
75S	Qoa (dacite clasts in hyperconcentrated flood deposit)	0.84	63.74	16.38	0.619	4.42	0.085	5.08	2.49	1.96	4.10	0.175	99.05
79P1	Qoa (dacite clasts in hyperconcentrated flood deposit)	0.78	65.54	16.22	0.567	3.66	0.077	4.49	1.96	2.14	4.26	0.151	99.06
79P2	Qoa (dacite clasts in hyperconcentrated flood deposit)	0.62	65.02	16.27	0.567	3.82	0.078	4.65	2.16	2.07	4.20	0.156	98.99
79P2-2	Qoa (dacite clasts in hyperconcentrated flood deposit)	0.53	64.60	16.45	0.573	4.17	0.080	4.70	2.10	2.05	4.25	0.163	99.14
79P2-3	Qoa (dacite clasts in hyperconcentrated flood deposit)	1.16	65.71	16.05	0.534	3.75	0.075	4.32	1.88	2.18	4.22	0.150	98.86

B. GEOCHEMICAL DATA (continued)

MAJOR ELEMENTS NORMALIZED RESULTS (WEIGHT PERCENT)

Sample no.	Geologic unit (rock type)	LOI (%)	SiO_2	Al_2O_3	TiO_2	FeO*	MnO	CaO	MgO	K_2O	Na_2O	P_2O_5	Total
HELENA–HAYSTACK MÉLANGE METAVOLCANIC ROCKS AND EASTON METAMORPHIC SUITE METAVOLCANIC ROCKS AND SEMISCHISTS													
2H2	Jph_j (semischistose metasandstone)	3.79	67.21	11.87	0.656	6.06	0.121	5.33	5.15	1.23	2.24	0.132	100
2K	Jmv_h (metabasaltic greenstone)	2.94	52.12	17.14	1.377	7.83	0.134	9.59	6.47	0.20	4.95	0.179	100
2K rerun	Jmv_h (metabasaltic greenstone)	2.94	52.22	17.19	1.382	7.67	0.134	9.61	6.46	0.20	4.94	0.178	100
2K avg.	Jmv_h (metabasaltic greenstone)	2.94	52.17	17.17	1.380	7.75	0.134	9.60	6.47	0.20	4.95	0.179	100
2O	Jsh_s (metabasaltic greenschist)	2.24	46.46	16.25	0.385	11.51	0.119	14.76	8.86	0.02	1.61	0.014	100
2P	Jsh_s (metabasaltic andesitic greenschist)	3.27	53.61	18.87	0.304	7.92	0.151	4.54	7.86	1.41	5.31	0.022	100
3A	$Jigb_h$ (metagabbroic greenstone)	2.65	50.11	15.10	1.697	10.32	0.193	9.58	8.22	1.38	3.23	0.161	100
4O	Jsh_s (metabasaltic greenschist)	2.48	47.86	16.46	0.679	12.65	0.212	11.26	8.20	0.36	2.30	0.018	100
6J	Jmv_h (metabasaltic greenstone)	3.20	51.15	16.33	2.041	8.88	0.151	8.05	7.73	1.43	3.96	0.284	100
12B	Jmv_h (metabasaltic andesitic greenstone)	2.31	54.72	15.11	1.890	8.53	0.250	6.60	6.29	0.15	6.26	0.200	100
12C	Jmv_h (metabasaltic greenstone)($Jigb_h$?)	2.54	51.00	19.12	1.627	11.49	0.210	6.31	3.98	0.02	6.02	0.225	100
15Q	$Jhmc_h$ (andesitic greenstone)(metatuff?)	4.77	61.59	16.26	0.520	7.57	0.265	3.37	4.06	0.02	6.25	0.093	100
15R	Jmv_h (metabasaltic greenstone)	3.03	49.71	14.01	1.641	10.66	0.223	12.91	7.15	0.03	3.52	0.147	100
16C	Jph_j (semischistose metasandstone)	2.91	68.60	14.35	0.739	7.72	0.101	0.68	3.03	0.92	3.70	0.162	100
24G	Jmv_h (tuffaceous andesitic greenstone)	3.20	66.70	14.91	0.494	3.86	0.197	11.27	1.62	0.42	0.40	0.146	100
24M	Jmv_h (metabasaltic greenstone)	2.56	49.26	14.27	2.350	14.89	0.256	8.94	5.52	0.03	4.26	0.226	100
24S	Jmv_h (metabasaltic greenstone)	2.01	51.47	12.98	2.576	12.29	0.255	8.68	6.66	0.94	3.90	0.258	100
25B	Ju_h (serpentinite)	10.35	33.35	19.49	1.814	15.64	0.311	1.59	27.64	0.00	0.00	0.161	100
25Z	Ju_h (diopside-bearing pyroxenite)	3.66	51.50	4.86	0.249	6.52	0.158	15.33	21.12	0.00	0.24	0.023	100
25Z2	Jmv_h (metabasaltic greenstone)	2.17	57.42	18.96	0.868	7.66	0.076	2.73	3.41	0.02	8.61	0.260	100
31AA1	Ju_h (serpentinite)	12.68	29.85	19.16	2.604	18.23	0.504	5.91	23.36	0.00	0.13	0.248	100
31AA1 rerun	Ju_h (serpentinite)	12.68	30.86	18.79	2.605	17.90	0.505	5.94	22.77	0.00	0.38	0.242	100
31AA1 avg.	Ju_h (serpentinite)	12.68	30.35	18.98	2.604	18.07	0.505	5.92	23.07	0.00	0.26	0.245	100
31AP1	Jsh_s (metabasaltic greenschist)	6.16	44.79	25.31	0.645	5.93	0.144	12.11	7.13	1.55	2.32	0.061	100
32A	Jmv_h (meta-andesitic greenstone)	3.29	58.43	14.43	0.787	9.81	0.213	8.21	3.29	0.25	4.48	0.105	100
34L	Jmv_h? (metabasaltic andesitic greenstone)	2.27	53.22	16.07	1.294	10.13	0.184	6.67	5.99	0.03	6.28	0.135	100
41R	Jsh_s (metabasaltic greenschist)	6.25	48.36	14.61	2.272	9.52	0.166	13.61	5.90	0.21	5.04	0.293	100
42Q	Jmv_h (meta-andesitic greenstone) (metatuff?)	2.81	58.44	16.31	0.760	9.70	0.188	4.02	4.54	0.34	5.59	0.117	100
46Q	Jsh_s (metabasaltic greenschist)	2.38	51.62	15.15	1.670	10.39	0.187	8.95	7.47	0.02	4.39	0.149	100

Sample no.	Geologic unit (rock type)	LOI (%)	SiO_2	Al_2O_3	TiO_2	FeO*	MnO	CaO	MgO	K_2O	Na_2O	P_2O_5	Total
47I	Jmv_h (metabasaltic greenstone breccia)	3.78	50.28	15.09	2.384	12.30	0.217	7.72	7.08	0.10	4.59	0.238	100
47J	Jmv_h (metabasaltic andesitic greenstone)	2.35	52.45	14.34	1.756	10.27	0.194	8.24	7.39	0.09	5.09	0.180	100
50C	Jsh_s (metabasaltic andesitic greenschist)	6.05	53.87	16.38	1.411	11.29	0.283	5.24	10.27	0.00	1.15	0.111	100
50D	Jsh_s (metabasaltic andesitic greenschist)	2.22	56.73	17.11	0.888	7.34	0.129	5.34	5.03	0.03	7.21	0.191	100
50I	Jsh_s (andesitic greenschist) (metatuff?)	3.78	59.16	17.38	0.583	8.79	0.182	3.20	5.30	0.02	5.30	0.092	100
56W	Jph_j (semischistose metasandstone)	2.66	69.43	14.31	0.865	6.45	0.104	0.25	3.11	0.73	4.57	0.177	100
59M	Jph_j (semischistose metasandstone)	2.67	73.17	12.54	0.615	5.75	0.107	0.47	2.80	1.00	3.45	0.099	100
68H	Jsh_s (metabasaltic greenschist)	1.45	46.24	14.98	1.382	11.63	0.203	16.67	7.62	0.02	1.15	0.108	100
68I	Jsh_s (metabasaltic greenschist)	1.45	48.10	15.27	0.361	10.42	0.114	15.51	8.59	0.01	1.62	0.013	100
69S	Jsh_s (protomylonitized metabasaltic greenschist)	2.88	50.36	14.59	3.209	13.74	0.244	6.03	6.66	0.02	4.79	0.366	100
U-Pb2	$Jigb_h$ (metagabbroic greenstone)	2.31	51.48	15.30	1.745	8.92	0.175	11.67	5.97	0.04	4.58	0.114	100
DACITE													
42P1	Qoa (dacite clasts in hyperconcentrated flood deposit)	0.62	64.53	16.65	0.59	4.32	0.08	4.92	2.35	1.96	4.44	0.158	100
42P2	Qoa (dacite clasts in hyperconcentrated flood deposit)	0.90	63.95	16.75	0.59	4.39	0.09	5.08	2.54	1.91	4.55	0.157	100
42P3	Qoa (dacite clasts in hyperconcentrated flood deposit)	0.72	63.81	17.01	0.59	4.29	0.08	5.24	2.49	1.87	4.46	0.153	100
75S	Qoa (dacite clasts in hyperconcentrated flood deposit)	0.84	64.35	16.54	0.625	4.46	0.086	5.13	2.51	1.98	4.14	0.177	100
79P1	Qoa (dacite clasts in hyperconcentrated flood deposit)	0.78	66.16	16.37	0.572	3.69	0.078	4.53	1.98	2.16	4.30	0.152	100
79P2	Qoa (dacite clasts in hyperconcentrated flood deposit)	0.62	65.69	16.44	0.573	3.85	0.079	4.70	2.18	2.09	4.24	0.158	100
79P2-2	Qoa (dacite clasts in hyperconcentrated flood deposit)	0.53	65.16	16.59	0.578	4.21	0.081	4.74	2.12	2.07	4.29	0.164	100
79P2-3	Qoa (dacite clasts in hyperconcentrated flood deposit)	1.16	66.46	16.23	0.540	3.79	0.076	4.37	1.90	2.21	4.27	0.152	100

B. GEOCHEMICAL DATA (continued)

RARE EARTH ELEMENTS UNNORMALIZED RESULTS (WEIGHT PERCENT)

Sample no.	Geologic unit (rock type)	La	Ce	Pr	Nd	Sm	Eu	Gd	Tb	Dy	Ho	Er	Tm	Yb	Lu	Ba	Th	Nb	Y	Hf	Ta	U	Pb	Rb	Cs	Sr	Sc
HELENA–HAYSTACK MÉLANGE METAVOLCANIC ROCKS AND EASTON METAMORPHIC SUITE METAVOLCANIC ROCKS AND SEMISCHISTS																											
2H2	Jph_j (semischistose metasandstone)	8.13	17.1	2.17	9.91	2.83	0.8	3.08	0.51	3.26	0.66	1.78	0.27	1.61	0.26	416	1.71	3.41	18.48	1.87	0.22	0.64	2.91	27.3	1.27	239	26.9
2K	Jmv_h (metabasaltic greenstone)	6.74	15.65	2.03	9.74	3.28	1.19	3.75	0.64	4.32	0.89	2.27	0.33	2.07	0.3	38	1	6.78	21.83	2.28	0.46	0.23	0.83	3.1	0.22	143	35.6
2O	Jsh_s (metabasaltic greenschist)	0.5	0.74	0.15	0.79	0.35	0.18	0.55	0.1	0.67	0.14	0.38	0.05	0.29	0.05	18	0.09	0.1	3.42	0.11	0.01	0.01	0.44	0.6	0.02	546	57.2
2P	Jsh_s (metabasaltic andesitic greenschist)	0.69	2.17	0.38	2.12	0.91	0.39	1.28	0.24	1.62	0.36	0.96	0.14	0.9	0.13	579	0.03	0.42	8.6	0.36	0.03	0.01	0.69	28	0.78	125	46.2
3A	$Jigb_h$ (metagabbroic greenstone)	4.16	11.59	1.81	9.92	3.82	1.37	5.23	0.99	6.48	1.42	3.85	0.56	3.44	0.53	513	0.25	3.14	37.66	2.65	0.22	0.09	0.55	31.2	1.24	105	56.3
4O	Jsh_s (metabasaltic greenschist)	0.92	1.51	0.25	1.13	0.45	0.29	0.65	0.13	0.83	0.18	0.49	0.07	0.46	0.07	61	0.1	0.11	4.78	0.14	0.01	0.03	0.89	3.8	0.19	959	48.7
6J	Jmv_h (metabasaltic greenstone)	13.16	27.88	3.61	16.33	4.71	1.69	5.54	0.96	5.82	1.19	3.2	0.45	2.74	0.42	230	1.26	16.72	32.73	3.56	1.06	0.39	1.1	20.8	1.61	236	48.7
12B	Jmv_h (metabasaltic andesitic greenstone)	4.74	13.05	2.06	10.72	4.29	1.46	5.52	1	6.8	1.44	3.76	0.53	3.4	0.51	274	0.3	3.97	33.79	3.01	0.29	0.51	0.4	3.5	0.17	136	44
12C	Jmv_h (metabasaltic greenstone)($Jigb_h$?)	4.72	11.47	1.7	9.11	3.33	1.27	4.01	0.68	4.76	0.97	2.47	0.37	2.28	0.35	17	0.25	3.47	22.35	1.96	0.22	0.12	0.59	0.3	0.04	330	40.5
15Q	$Jhmc_h$ (andesitic greenstone)(metatuff?)	4.42	8.3	1.13	5.71	1.92	0.65	2.3	0.38	2.82	0.59	1.62	0.24	1.6	0.24	30	0.51	0.5	15.07	0.96	0.03	0.21	0.63	0.5	0.04	134	31.4
15R	Jmv_h (metabasaltic greenstone)	3.79	10.6	1.7	9.42	3.77	1.52	5.16	0.93	6.57	1.38	3.6	0.55	3.4	0.52	12	0.19	2.39	34.17	2.69	0.19	0.42	0.81	0.6	0.04	130	53.2
16C	Jph_j (semischistose metasandstone)	12.79	24.88	3.07	13.06	3.4	0.9	3.41	0.55	3.35	0.68	1.84	0.27	1.65	0.27	264	3.63	6.16	18.59	3.1	0.46	1.4	9.32	28.7	1.99	36	16.8
24G	Jmv_h (tuffaceous andesitic greenstone)	12.08	28.61	3.94	17.3	4.77	1.26	4.66	0.79	5.09	1.1	3.04	0.44	2.91	0.46	149	1.94	2	28.18	3.64	0.14	0.74	4.74	5.3	0.22	87	15.1
24M	Jmv_h (metabasaltic greenstone)	3.05	9.24	1.56	9.42	4.29	1.51	5.97	1.08	7.57	1.62	4.2	0.61	3.98	0.59	45	0.12	3.06	37.31	1.46	0.23	0.04	0.66	0.5	0.24	79	48.4
24S	Jmv_h (metabasaltic greenstone)	5.61	16.1	2.59	14.8	5.62	1.75	7.71	1.4	9.6	2.01	5.42	0.83	5.12	0.79	206	0.34	4.83	52.2	4.45	0.37	0.38	0.6	14.2	2.04	108	50.6
25B	Ju_h (serpentinite)	2.52	9.75	1.77	9.94	3.85	1.67	5.26	0.99	6.62	1.46	3.95	0.56	3.52	0.52	3	0.25	2.35	37.18	2.57	0.17	0.16	0.22	0.2	0.06	9	51.3
25Z	Ju_h (diopside-bearing pyroxenite)	1.02	2.31	0.38	1.89	0.79	0.28	1.04	0.2	1.39	0.3	0.81	0.12	0.89	0.15	7	0.21	0.35	7.14	0.52	0.03	0.07	0.75	0.1	0.22	13	43.7
25Z2	Jmv_h (metabasaltic greenstone)	15.96	33.72	4.24	18.26	4.76	1.2	4.57	0.79	5.02	1.04	2.89	0.43	2.83	0.44	19	5.74	7.21	26.86	3.92	0.53	1.76	3.64	0.2	0.04	452	27.8
31AA1	Ju_h (serpentinite)	5.42	13.64	2.23	12.57	4.72	2	6.41	1.24	8.18	1.76	4.88	0.72	4.5	0.73	24	0.52	4.34	47.53	3.43	0.29	0.77	0.71	0.1	0.3	208	65.8
31AP1	Jsh_s (metabasaltic greenschist)	1.78	4.91	0.79	4.26	1.59	0.75	2.15	0.41	2.72	0.59	1.54	0.22	1.4	0.22	389	0.15	0.88	15.16	1.01	0.06	0.04	0.31	37.5	1.83	35	24.4
32A	Jmv_h (meta-andesitic greenstone)	4.66	9.4	1.43	7.09	2.46	0.81	3.12	0.61	3.98	0.89	2.49	0.37	2.36	0.38	176	0.78	0.99	22.27	1.63	0.07	0.26	2.97	8.3	10.84	30	36.9
32A rerun	Jmv_h (meta-andesitic greenstone)	4.77	9.51	1.43	7.1	2.58	0.83	3.31	0.61	4.04	0.89	2.48	0.37	2.35	0.38	178	0.78	1.04	23.47	1.63	0.07	0.25	2.75	9	10.8	31	40.6

Sample no.	Geologic unit (rock type)	La	Ce	Pr	Nd	Sm	Eu	Gd	Tb	Dy	Ho	Er	Tm	Yb	Lu	Ba	Th	Nb	Y	Hf	Ta	U	Pb	Rb	Cs	Sr	Sc
32A avg.	Jmv_h (meta-andesitic greenstone)	4.72	9.46	1.43	7.09	2.52	0.82	3.21	0.61	4.01	0.89	2.49	0.37	2.35	0.38	177	0.78	1.01	22.87	1.63	0.07	0.26	2.86	8.61	10.82	30.79	38.73
34L	Jmv_h? (metabasaltic andesitic greenstone)	5.06	11.5	1.73	9.18	3.18	1.06	4.01	0.77	5.13	1.12	3.11	0.45	2.89	0.46	48	0.56	2.19	29.09	2.21	0.15	0.22	1.15	0.5	0.06	264	39.1
41R	Jmv_h (metabasaltic greenstone)	11.18	26.74	3.57	16.98	5.19	1.8	5.7	0.99	6.13	1.28	3.29	0.47	2.78	0.43	23	0.72	10.94	32.66	4.05	0.78	0.28	1.49	2.8	0.31	265	45.7
42Q	Jmv_h (meta-andesitic greenstone) (metatuff?)	4.01	9.67	1.49	7.67	2.54	0.74	3.01	0.53	3.51	0.78	2.14	0.33	2.1	0.35	244	0.64	0.67	20.45	1.42	0.05	0.25	1.4	4.7	0.95	134	43.2
46Q	Jsh_s (metabasaltic greenschist)	3.75	10.88	1.77	9.72	3.82	1.29	4.95	0.97	6.31	1.38	3.7	0.53	3.34	0.52	16	0.21	2.53	35.58	2.54	0.18	0.09	1.25	0.2	0.01	252	50.6
47I	Jmv_h (metabasaltic greenstone breccia)	7.75	19.15	2.74	13.94	4.95	1.72	6.41	1.22	7.87	1.66	4.57	0.65	4.11	0.64	68	0.65	8.27	45.22	3.47	0.53	0.35	0.76	2.4	1.11	76	52.5
47J	Jmv_h (metabasaltic andesitic greenstone)	5.68	14.01	2.02	10.79	4.07	1.4	5.33	1.01	6.81	1.46	3.93	0.56	3.45	0.53	44	0.5	6.15	38	2.82	0.41	0.24	0.76	1.8	1	77	49.3
50C	Jsh_s (metabasaltic andesitic greenschist)	2.85	8.55	1.46	8.11	3.13	1.16	4.37	0.86	5.64	1.26	3.48	0.5	3.11	0.5	5	0.08	1.05	34.22	2.05	0.08	0.31	1.84	0.1	0.03	27	50.9
50D	Jsh_s (metabasaltic andesitic greenschist)	4.5	11.01	1.62	8.68	3.04	1.14	4	0.74	4.98	1.07	2.98	0.45	2.83	0.46	14	0.33	3.24	28.85	2.87	0.2	0.13	0.49	0.1	0.02	150	26.7
50I	Jsh_s (andesitic greenschist) (metatuff?)	4.38	9.32	1.4	6.94	2.15	0.73	2.48	0.44	2.95	0.64	1.81	0.28	1.78	0.3	18	0.64	0.64	17.89	1.45	0.04	0.26	1.47	0.6	0.1	166	34.2
56W	Jph_j (semischistose metasandstone)	10.79	19.64	2.21	9.1	2.14	0.61	1.99	0.32	1.98	0.4	1.13	0.17	1.13	0.19	334	3.12	5.48	10.29	2.69	0.39	1.1	5.41	28	1.54	45	14.9
59M	Jph_j (semischistose metasandstone)	8.87	24.37	2.09	8.5	2.11	0.55	2	0.39	2.53	0.58	1.73	0.26	1.71	0.28	212	3.85	6.58	15.21	3.53	0.42	1.35	6.35	22.3	1.31	31	17.9
68H	Jsh_s (metabasaltic greenschist)	2.73	7.5	1.28	7.35	3.07	1.28	4.19	0.78	5.28	1.14	3.09	0.45	2.8	0.43	16	0.05	2.16	28.82	1.47	0.15	0.02	1.84	0.4	0.01	779	56.1
68I	Jsh_s (metabasaltic greenschist)	0.49	0.68	0.17	0.81	0.36	0.2	0.56	0.11	0.72	0.15	0.39	0.05	0.32	0.05	15	0.02	0.1	3.43	0.12	0.01	0	0.19	0.4	0.01	484	55.7
69S	Jsh_s (protomylonitized metabasaltic greenschist)	7.57	21.49	3.41	18.61	7.06	2.14	8.68	1.66	10.89	2.35	6.35	0.94	5.99	0.9	21	0.46	7.08	56.46	5.54	0.53	0.28	0.79	0.3	0.24	158	50.5
U-Pb2	$Jigb_h$ (metagabbroic greenstone)	3.2	9.22	1.52	8.35	3.24	1.24	4.43	0.82	5.46	1.16	3.26	0.48	2.89	0.46	67	0.17	2.58	31.66	2.35	0.19	0.06	0.28	1.6	0.07	99	50.8
DACITE CLASTS IN OLDER ALLUVIUM																											
42P1	Qoa (dacite clasts in hyperconcentrated flood deposit)	15.16	29.79	3.34	13.17	2.95	0.88	2.64	0.43	2.65	0.55	1.48	0.22	1.43	0.23	469	5.07	5.32	14.99	3.38	1.99	1.69	8.96	35.3	1.49	460	11.8
42P2	Qoa (dacite clasts in hyperconcentrated flood deposit)	14.73	28.45	3.26	13.28	2.96	0.92	2.68	0.44	2.59	0.55	1.47	0.22	1.46	0.24	457	4.67	5.28	14.98	3.32	2.36	1.65	8.71	33.8	1.42	474	12.4
42P3	Qoa (dacite clasts in hyperconcentrated flood deposit)	14.27	27.99	3.14	12.27	2.78	0.87	2.44	0.41	2.54	0.52	1.43	0.21	1.35	0.22	446	4.64	4.9	14.35	3.03	0.91	1.57	8.43	33.6	1.37	483	12
75S	Qoa (dacite clasts in hyperconcentrated flood deposit)	16.83	33.4	3.81	15.36	3.52	1	3.13	0.51	2.98	0.62	1.65	0.24	1.6	0.26	476	4.98	5.3	16.29	3.64	0.42	1.7	8.77	36.1	1.44	501	13.9
79P1	Qoa (dacite clasts in hyperconcentrated flood deposit)	17.37	33.49	3.74	14.71	3.09	0.94	2.78	0.45	2.64	0.54	1.47	0.22	1.45	0.25	514	5.64	5.06	14.94	3.6	0.43	1.96	11.72	40.2	1.68	498	10.4
79P2	Qoa (dacite clasts in hyperconcentrated flood deposit)	16.45	31.52	3.46	13.82	3.08	0.93	2.77	0.45	2.72	0.55	1.47	0.22	1.51	0.24	494	5.02	5.03	14.67	3.52	0.42	1.77	11.92	38	1.54	472	11
79P2-2	Qoa (dacite clasts in hyperconcentrated flood deposit)	16.6	31.97	3.61	14.27	3.13	0.93	2.79	0.44	2.73	0.55	1.5	0.22	1.43	0.24	510	5.3	5.02	14.99	3.53	0.43	1.76	10.97	38.1	1.58	484	11.1

B. GEOCHEMICAL DATA (continued)

TRACE ELEMENT (PPM)

Sample no.	Geologic unit (rock type)	LOI (%)	Ni	Cr	Sc	V	Ba	Rb	Sr	Zr	Y	Nb	Ga	Cu	Zn	Pb	La	Ce	Th
HELENA–HAYSTACK MÉLANGE METAVOLCANIC ROCKS AND EASTON METAMORPHIC SUITE METAVOLCANIC ROCKS AND SEMISCHISTS																			
2H2	Jph_j (semischistose metasandstone)	3.79	101	173	19	152	428	28	241	73	17	3.2	11	11	68	1	6	16	2
2K	Jmv_h (metabasaltic greenstone)	2.94	62	208	33	197	22	3	147	97	22	7.7	13	80	57	0	18	13	0
2K rerun	Jmv_h (metabasaltic greenstone)	2.94	61	215	34	195	17	2	147	97	21	8.3	16	80	54	0	0	23	3
2K avg.	Jmv_h (metabasaltic greenstone)	2.94	62	212	34	196	20	2	147	97	22	8.0	14	80	56	0	9	18	2
2O	Jsh_s (metabasaltic greenschist)	2.24	27	51	44	470	28	0	522	27	3	0.0	16	49	21	0	0	7	0
2P	Jsh_s (metabasaltic andesitic greenschist)	3.27	54	79	40	158	668	33	123	18	8	1.5	13	32	73	0	0	12	0
3A	$Jigb_h$ (metagabbroic greenstone)	2.65	75	307	43	330	537	32	97	93	34	3.1	17	66	86	1	20	12	4
4O	Jsh_s (metabasaltic greenschist)	2.48	26	44	42	546	81	1	948	42	4	0.2	17	301	74	2	6	8	2
6J	Jmv_h (metabasaltic greenstone)	3.20	46	202	36	271	204	21	226	140	30	17.6	18	79	69	2	9	36	1
12B	Jmv_h (metabasaltic andesitic greenstone)	2.31	116	266	40	318	247	2	120	114	34	4.6	17	40	69	0	0	16	2
12C	Jmv_h (metabasaltic greenstone)($Jigb_h$?)	2.54	0	9	30	215	0	0	384	92	23	5.0	20	16	72	0	6	27	3
15Q	$Jhmc_h$ (andesitic greenstone; metatuff?)	4.77	5	27	28	190	36	1	145	32	14	0.3	18	75	74	0	0	7	2
15R	Jmv_h (metabasaltic greenstone)	3.03	53	160	44	349	0	0	126	91	33	2.5	18	57	85	1	8	16	6
16C	Jph_j (semischistose metasandstone)	2.91	50	99	16	148	267	30	35	108	20	6.7	14	52	127	7	18	32	3
24G	Jmv_h (tuffaceous andesitic greenstone)	3.20	10	15	19	85	158	7	87	126	29	2.3	18	53	53	5	6	33	2
24M	Jmv_h (metabasaltic greenstone)	2.56	4	54	41	440	11	0	82	52	39	3.8	20	21	124	0	6	13	1
24S	Jmv_h (metabasaltic greenstone)	2.01	37	94	44	444	218	17	117	148	51	5.2	19	28	106	0	3	32	2
25B	Ju_h (serpentinite)	10.35	521	952	43	384	0	0	10	96	40	3.1	12	70	116	1	0	12	3
25Z	Ju_h (diopside-bearing pyroxenite)	3.66	180	567	44	146	18	1	12	19	7	1.5	7	7	41	0	5	2	2
25Z2	Jsh_s (metabasaltic greenstone)	2.17	55	120	21	222	3	1	434	141	26	7.8	22	55	122	2	0	50	5
31AA1	Ju_h (serpentinite)	12.68	59	149	56	551	0	0	205	143	54	7.0	19	156	249	0	4	13	5
31AA1 rerun	Ju_h (serpentinite)	12.68	61	146	53	532	0	0	207	145	54	6.6	21	244	290	0	10	14	1
31AA1 avg.	Ju_h (serpentinite)	12.68	60	148	54	542	0	0	206	144	54	6.8	20	200	270	0	7	14	3
31AP1	Jsh_s (metabasaltic greenschist)	6.16	120	247	25	129	371	38	36	39	15	1.3	14	35	43	0	2	0	0
32A	Jmv_h (meta-andesitic greenstone)	3.29	20	49	39	366	196	9	30	50	21	1.6	17	61	89	0	10	12	0
34L	Jmv_h? (metabasaltic andesitic greenstone)	2.27	35	109	32	285	39	0	291	84	30	2.5	15	70	94	0	0	21	2
41R	Jsh_s (metabasaltic greenschist)	6.25	33	83	41	322	0	2	317	164	31	11.3	18	51	78	0	22	54	2
42Q	Jmv_h (meta-andesitic greenstone) (metatuff?)	2.81	6	28	31	277	243	4	131	49	20	0.3	17	79	81	0	5	22	1
46Q	Jsh_s (metabasaltic greenschist)	2.38	68	243	40	347	0	0	256	100	34	2.6	18	8	77	0	0	22	3

Sample no.	Geologic unit (rock type)	LOI (%)	Ni	Cr	Sc	V	Ba	Rb	Sr	Zr	Y	Nb	Ga	Cu	Zn	Pb	La	Ce	Th
47I	Jmv_h (metabasaltic greenstone breccia)	3.78	33	71	45	413	40	2	78	131	46	9.7	21	63	102	0	0	29	1
47K	Jmv_h (metabasaltic andesitic greenstone)	2.35	45	101	39	345	27	1	75	94	34	7.1	17	65	96	0	0	18	1
50C	Jsh_s (metabasaltic andesitic greenschist)	6.05	87	347	43	299	0	0	30	73	32	1.5	21	33	76	6	10	17	2
50D	Jsh_s (metabasaltic andesitic greenschist)	2.22	31	63	26	169	0	0	129	100	25	4.5	15	58	57	0	2	20	1
50I	Jsh_s (andesitic greenschist; metatuff?)	3.78	15	54	23	221	25	1	151	52	17	1.6	20	44	69	5	5	19	0
56W	Jph_j (semischistose metasandstone)	2.66	52	174	14	172	212	24	30	131	15	7.6	15	22	101	2	6	42	2
59M	Jph_j (semischistose metasandstone)	2.67	60	199	11	111	341	29	45	96	11	6.3	13	19	82	5	15	24	3
68H	Jsh_s (metabasaltic greenschist)	1.45	57	333	47	404	0	0	826	78	27	1.8	22	21	60	3	12	13	4
68I	Jsh_s (metabasaltic greenschist)	1.45	24	52	47	461	28	0	464	26	4	0.5	15	36	19	0	0	7	4
69S	Jsh_s (protomylonitized metabasaltic greenschist)	2.88	43	122	46	450	0	0	160	197	57	6.7	19	56	117	0	0	22	1
U-Pb2	$Jigb_h$ (metagabbroic greenstone)	2.31	47	120	41	376	36	1	96	78	29	1.9	18	14	54	0	3	20	1
DACITE																			
42P1	Qoa (dacite clasts in hyperconcentrated flood deposit)	0.62	19	21	14	90	486	36	462	141	15	6.6	17	7	54	8	18	25	6
42P2	Qoa (dacite clasts in hyperconcentrated flood deposit)	0.90	22	18	14	86	471	34	474	135	14	5.2	19	6	56	7	25	41	7
42P3	Qoa (dacite clasts in hyperconcentrated flood deposit)	0.72	24	28	13	85	454	34	478	127	15	4.8	17	6	57	4	11	36	3
75S	Qoa (dacite clasts in hyperconcentrated flood deposit)	0.84	22	23	17	89	476	35	508	141	16	5.1	17	7	56	5	13	45	3
79P1	Qoa (dacite clasts in hyperconcentrated flood deposit)	0.78	17	16	9	80	539	41	481	143	15	5.1	18	9	53	12	20	37	4
79P2	Qoa (dacite clasts in hyperconcentrated flood deposit)	0.62	20	18	11	83	508	39	449	140	15	4.8	16	10	57	9	6	52	4
79P2-2	Qoa (dacite clasts in hyperconcentrated flood deposit)	0.53	19	17	14	76	495	38	502	143	15	5.3	15	6	55	9	17	26	3
79P2-3	Qoa (dacite clasts in hyperconcentrated flood deposit)	1.16	17	15	10	71	531	42	467	146	14	4.9	17	7	49	8	16	45	4